Academic Year 2018-2019

Faculty Pharmaceutical, Biomedical and Veterinary Sciences

Biomedical Sciences

Phyllosphere bacteria: potential for degradation of indoor air pollutants and impact on the human immune response to air pollutants

By:

Max Dekeukeleire

Project proposal in partial fulfillment of the requirements for the degree
Master in Biomedical Sciences

Promotor: Prof. Dr. ir. Sarah Lebeer

Coach: Dr. ir. Wenke Smets

Research group Environmental Ecology & Applied Microbiology

Campus Groenenborger

Gebouw V, Verdieping 5

Groenenborgerlaan 171

Table of contents

Preface

With this master thesis, I am finishing the programme of Biomedical sciences, Master in Environmental Health sciences at the University of Antwerp. During the past 8 months, I have worked on this project. However without a few a people, I wouldn't have succeeded this journey and therefore, they deserve my gratitude.

I am grateful to my supervisors Professor Sarah Lebeer and Dr Wenke Smets for giving me the opportunity to undertake my master thesis in their Lab of Applied Microbiology and Biotechnology within the ENdEMIC research group. Thanks to them, I was able to discover a very interesting topic in a heart-warming lab.

I am thankful for the continuous support, guidance and mentoring of Dr Wenke Smets throughout the duration of my thesis, teaching me everything I need to know in the laboratory, making time for me when experiments lasted longer than working hours, and all the fun times during the badminton sessions and the cinema-trip.

A special thanks goes to Dr. Irina Spacova and Dr. Serena Moretti, for figuring out, setting up and assisting me in the human cell experiments and to Marie Legein for assisting me in the DNA-isolation and identification of the bacteria obtained from the liquid manure.

I also want to thank the Sustainable Energy, Air and Water Technology Group (DUEL) for making their gas chromatograph available during my thesis and the Lab of Environmental and Urban Ecology for their guidance and for the usage of their measuring equipment during the SIRM measurements.

I would like to thank Tom Tytgat and Katrien Michiels for the guidance in the installation of the multichannel gas sensor.

Next, I want to thank my father for driving me around during the field work.

Last but not least, I would like to thank my co-readers Hans Keune and Jan Cools for their time to read and evaluate my thesis.

Thank you UAntwerpen and ENdEMIC research group,

Max Dekeukeleire.

Abbreviations

ABC	ATP binding cassette
ANOVA	Analysis of variance
BTEX	Benzene, toluene, ethylbenzene, and xylene
BTF	Biotrickling filter
CFU	Colony forming units
DALY	Disability adjusted life years
DAMPs	Damage-associated molecular patterns
DEP	Diesel exhaust particles
DNRA	Dissimilatory nitrite reduction to ammonium
GC	Gas chromatograph
IAIAQ	The International Association for Indoor Air Quality
LPS	Lipopolysaccharide
LTA	Lipoteichoic acids
MAMPs	Microbe-associated molecular patterns
MGS	Multichannel gas sensor
MM	Mineral salt medium
NF-kβ	Nuclear factor kappa B
NMDS	Nonmetric multidimensional scaling
NNP	Nitrate/nitrite porter
OD	Optical density
PAH	Polyaromatic hydrocarbons
PM	Particulate matter
pNPP	Para-Nitrophenylphosphate
PRRs	Pattern recognition receptors
R2A	Reasoner's 2A
SIRM	Saturation isothermal remanent magnetisation
SRM-1650b	Standard reference material-1650b
THP1-Dual cell	NF-kB-SEAP and IRF-Lucia luciferase Reporter Monocytes
TLRs	Toll-like receptors
Treg	Regulatory T cells
VOCs	Volatile organic compounds
WHO	World Health Organisation

Samenvatting

In de afgelopen decennia is er een toenemende bezorgdheid over de luchtvervuiling en de mogelijke schadelijke effecten die het met zich meebrengt. Aangezien de bevolking 90% van hun tijd binnenshuis doorbrengt, wordt de algehele blootstelling aan milieuvervuiling in grote mate bepaald door het binnenmilieu. Luchtverontreinigende stoffen, zoals vluchtige organische stoffen (VOS) en anorganische stikstof oxides (NO_X), kunnen zich binnenshuis accumuleren via lokale bronnen en via de buitenlucht. In deze context werd de capaciteit van fyllosfeer bacteriën om urbane luchtvervuiling in de binnenlucht te biodegraderen bestudeerd. Fyllosfeer bacteriën zijn bacteriën die de bovengrondse plantoppervlakken koloniseren. In deze studie werd de degradatie capaciteit van fyllosfeer bacteriën, geïsoleerd uit klimop en brandnetelgier, om de typische stedelijke (binnenshuis) luchtverontreinigende stoffen benzeen, tolueen, ethylbenzeen, xyleen (BTEX) en NOx te degraderen bestudeerd. Resultaten werden bekomen met behulp van de "Tolbox", een luchtdichte doos verbonden met een gaschromatografiesysteem en een meerkanaals gassensor die respectievelijk de gasvormige BTEX- en NOx-concentratie meet. Om de effectiviteit van deze bioremediatie capaciteit te beoordelen, werden de afbraaksnelheden door fyllosfeer bacteriën gekwantificeerd met behulp van deze opstelling. Daarnaast werd de impact van fyllosfeer bacteriën op het menselijke immuunrespons onderzocht en het vermogen om de interactie tussen diesel uitlaat partikels en de immuunrespons te moduleren bestudeerd. Dit werd geëvalueerd door NF-kB-SEAP en IRF-Lucia luciferase Reporter Monocyten, welke NF-KB blootstellen bij inductie, bloot te stellen aan fyllosfeer bacteriën, en/of diesel partikels (DEP).
Van de 17 geteste bacteriën werd één interessant bacterie, namelijk isolaat F, geïdentificeerd, die een indicatie gaf om benzene, toluene en xylene te degraderen. De blootstelling van fyllosfeer bacteriën aan THP1-dual cellen induceerde verschillende niveaus van NF-kb-productie waarbij *Methylbium petroleiphilum* en *Leuconostoc mesenteroides* de sterkste reactie induceerde. DEP bleken de interactie tussen fyllosfeer bacteriën en THP1-dual cellen te beïnvloeden. De toevoeging van DEP aan sterke immuun-inducerende bacteriën verminderde de NF-KB-productie in de THP1-dual cellen, terwijl toevoeging van DEP aan zwak immuun-inducerende bacteriën resulteerde in een toename van de productie van NF-kB. De resultaten van dit onderzoek bevestigen het pro-inflammatoire en immunosuppressieve effect van DEP zoals vermeld in de literatuur. De uitkomst van dit onderzoek kan bijdragen aan de ontwikkeling van nieuwe phylloremediatie toepassingen en in het begrijpen van de rol van de fyllosfeer bacterie en immuunsysteem-interactie in de menselijke gezondheid in relatie tot de luchtverontreiniging.

Abstract

The concern that urban air pollution, is a severe environmental problem is growing, because of our increasing knowledge on how it affects human health and well-being. Air pollutants, like volatile organic compounds (VOCs) and NO_X, can accumulate indoors and pose a major health problem as the population spends 90% of their time indoors. In this context, the involvement of phyllosphere bacteria in modulating the immune response and their applicability to biodegrade air pollution were studied. Phyllosphere bacteria are bacteria which can be found on aerial plant surfaces, mostly leaves. In this study, we identified phyllosphere bacteria from Ivy and liquid manure. The bioremediation of typical (indoor) urban air pollutants benzene, toluene, ethylbenzene, xylene (BTEX), and NO_x was investigated using the "Tolbox", which is an airtight chamber connected to a gas chromatography system and a multichannel gas sensor. To assess the effectivity of this bioremediation application, the biodegradation rates by phyllosphere bacteria were quantified using this setup. Furthermore, the impact of phyllosphere bacteria on the human immune response to air pollutants and the potential to modulate the interaction of particulate matter and the immune-response were evaluated by exposing NF-kB-SEAP and IRF-Lucia luciferase Reporter Monocytes (THP1-Dual cells) to phyllosphere bacteria and diesel particulate matter (DEP) and quantify the immune reaction by measuring the produced SEAP reporter, a reporter for NF-kb production. From the 17 tested bacteria, one interesting bacteria isolate F was identified to bioremediate TEX. Exposure of phyllosphere bacteria to THP1-Dual cells induced different levels of NF-kb production of which Methylibium petroleiphilum and Leuconostoc mesenteroides were identified to induce the strongest reaction. Diesel exhaust particles were found to influence this interaction between phyllosphere bacteria and THP1 dual cells. The addition of DEP to strong immune-inducing bacteria reduced the NF-kB production in THP1-Dual cells, while the addition of DEP to weak immune-inducing bacteria resulted in an increase of NF-kB production in THP1-Dual cells. The results of this study confirm the pro-inflammatory and immunosuppressive effect of DEP stated in literature. The outcome of this study may contribute to the development of new phylloremediation applications and to the understanding of the role of human-phyllosphere bacteria interaction in human health in relation to air pollution.

Chapter 1: literature review

1.1. Air pollutants and their health impact

Over the past decades, there is a growing concern about the air quality and potential deleterious effects of air pollution (Franklin et al., 2015, De Kempeneer et al., 2004). As the population spends 90% of their time indoors, the overall exposure to environmental pollution is to a large extent determined by the indoor environment. A range of indoor air pollutants like volatile organic compounds (VOCs) and NO_X, constitute a major indoor pollution problem (De Kempeneer et al., 2004, Sriprapat et al., 2014). The International Association for Indoor Air Quality (IAIAQ) reported in 2011 an overall 2 million disability adjusted life years (DALY) per year in Europe within a population of 480 million attributable to lower indoor air quality (Jantunen et al., 2011). This is more or equal to 3% of the total DALY due to all diseases from all causes in Europe (Jantunen et al., 2011). Urban areas typically consist of a high density of buildings and population in combination with a network of traffic routes, industries, power plants, etc., leading to a higher concentration of air pollution found in these areas (Eisner et al., 2009, Oltra et al., 2017). As result, the concentrations of pollutants in indoor air are often much more dangerous than those in the ambient outdoor air, as outdoor pollutants get diluted in the air due to dispersion (Masih et al., 2017, Hoge Gezondheidsraad, 2017). This is reflected in a report of the World Health Organisation (WHO) which states that indoor benzene concentration can vary between 0.6 to 3.4 times the concentration of outdoor benzene (World Health Organization, 2010b).

The Hoge Gezondheidsraad (2017) identified VOCs as one of the most significant groups of indoor contaminants in terms of DALY (27,776 DALY/year) (Hoge Gezondheidsraad, 2017, Jantunen et al., 2011). VOCs consist of a large number of compounds of air pollutants. in this study, the monocyclic aromatic hydrocarbons benzene, toluene, ethylbenzene, and isomers (m-, p-, o-) of xylene (BTEX) will be investigated together with nitrogen dioxide (NO_2) as major indoor air pollutants.

VOCs are found in a wide range of indoor environments as a result of their diversified and widespread indoor sources and their penetration from outside environments (El-Hashemy and Ali, 2018b). BTEX can originate from common household materials and products, involving coatings, dyes, detergents, varnishes, thinners, adhesives, degreasers, pesticides, lacquers, synthetic fragrances, nail polish, printing solvents, and petroleum derivatives (World Health Organization, 2010a, ATSDR, 2015, Sriprapat et al., 2014, Kandyala et al., 2010, ATSDR, 2010). In households with smokers, tobacco smoke is a major source of benzene, toluene, and ethylbenzene. Furthermore, xylene is emitted during the processing of rubber and leather in industries (Kandyala et al., 2010). Outdoors BTEX are mainly associated with motorized traffic emissions (Geiss et al., 2011), whereby 59% of the gasoline pollutant emission consists of BTEX (Padhi and Gokhale, 2017).

BTEX can pose a threat to human health and the environment when it is present in the air. Inhalation is, therefore, the main route of exposure. Exposure to BTEX is characterized by disruptive endocrine activity and by the impairment of the immune, metabolic, respiratory, and reproductive systems (Table 1 in appendix) (Tsangari et al., 2017, Dehghani et al., 2018, Wei et al., 2017). In addition, Benzene and ethylbenzene have been classified by the International Agency for Cancer Research as carcinogenic and possibly carcinogenic to humans, while toluene and xylene cannot be classified as carcinogenic for humans (IARC, 2018). Furthermore, BTEX pollutants can generate secondary pollutants such as ozone and secondary aerosols via gas-to-particle conversion processes leading to secondary health effects (Dehghani et al., 2018).

Nitrogen oxides (NO_x) are another major group of air pollutants. Nitric oxide (NO) and nitrogen dioxide (NO_2) are the two principal NO_x associated with fuel combustion taking place in vehicle engines, industrial facilities and domestic heating. The outdoor air concentration of NO and NO_2 mainly depend on the local sources and sinks. Annual mean concentrations of NO_2 in urban areas throughout the world are generally in the range of 20–90 µg/m^3, but there are occasions of combined NO and NO_2 in dense urban areas that exceed a total concentration of 500 µg/m^3 (World Health Organization, 2010b). In Flanders (Belgium), the regional average ranges from 19.7 µg/m³(Limburg) to 24.8 µg/m³ (province of Antwerp). In urbanized areas the average concentrations of pollutants are generally higher, for example the city of Antwerp has an average concentration of 33.8 µg/m³, with an average concentration measured in the city centre of 38.4 µg/m³ (Meysman and De Craemer, 2018). The outdoor air pollution contributes a major part to the indoor concentration as the indoor:outdoor ratio is between 0.88 and 1, if there are no indoor nitrogen dioxide sources present (World Health Organization, 2010b). The indoor air pollution can thus be further built up by indoor sources, like tobacco use, poorly maintained and unflued gas-, wood-, oil-, kerosene- and coal-burning systems and stoves. Maximum levels reported in European homes in association with these appliances are in the range of 180–2500 µg/m^3 (World Health Organization, 2010b). The WHO has published guidelines for indoor threshold value for NO_2 of 40 µg/m³ (annual) and for short-term exposure of 200 µg/m3 (1 h) (Salthammer et al., 2018). Increased NO_2 concentration can cause increased asthmatic bronchitis, reduced lung function growth, respiratory infections, airway obstruction, chronic phlegm, and rhinoconjunctivitis (Cibella et al., 2015, Wei et al., 2017). Metzger et al. (2004) found a 2.5% increase

of hospital admissions for respiratory disorders such as myocardial infarction and ischemic heart disease per 50 µg/m^3 increase of the NO_2 24-hour mean. Long term exposure could lead to reduced lung function in children (Gauderman et al., 2002) and cause lung cancer (Filleul et al., 2005).

1.2. Bioremediation of air

To date, various technological solutions to remove indoor air pollutants have yet been developed, whereby various air cleaning technologies, mostly rely on chemical, physical (incineration, filtration, adsorption or ionization) or photocatalytic oxidation techniques (Frost & Sullivan, 2016, Akmirza et al., 2017). However, as air cleaners can act as sinks for pollution, they are also sources of pollution. Air cleaners can generate their own pollutants via energy use and via by-products (e.g. intermediates) which lead to secondary pollution. Air purification systems tend to lose efficiency over time, have a high operation cost (Siegel, 2016), and are less affordable for common people (Frost & Sullivan, 2016). Altogether, these conventional air cleaners have their drawbacks leading to the need for the development of new cleaning technologies.

A more cost-effective, sustainable, natural, and eco-friendly alternative is bioremediation of air contaminants. Bioremediation uses micro-organisms to degrade, transform or assimilate environmental contaminants into less toxic or nontoxic forms (Wei et al., 2017). Bioremediation has already been applied in a wide variety of bioremediation techniques. These techniques can be divided into two overarching groups: *ex situ* and *in situ* bioremediation techniques. *Ex situ* techniques rely on transporting pollutants from polluted sites to another site for treatment while *in situ* techniques involve treating polluted substances at the site of pollution. Examples of *ex situ* techniques are respectively biopile, windrows, bioreactor, landfarming, and examples of *in situ* techniques are bioventing, bioslurping, biosparging, and phytoremediation. Phytoremediation is defined as the use of plants and associated micro-organisms to mitigate the toxic effects of pollutants via removal, stabilization, and degradation (Azubuike et al., 2016). The aforementioned example is mainly applied in the cleaning of contaminated soil. Biotrickling filter (BTF), bioscrubbers and biofilters are examples of air filters based on bioremediation (Fig. 1; Delhomenie and Heitz, 2005). These filters have a fixed-bed bioreactor, in which degrading micro-organisms are immobilized in biofilms to a packed bed. Contaminated air is pumped through the material, where pollutants diffuse into the biofilm synthesized by the microflora, and are degraded by the micro-organisms. BTF and bioscrubbers rely on recirculating water in which air pollutants get dissolved and are transported to a fixed-bed bioreactor. However, major limitations are the requirement of high maintenance, the generation of waste water and excess sludge, the need for energy input for forced air current, and the potential for vector and odour problems (Delhomenie and Heitz, 2005).

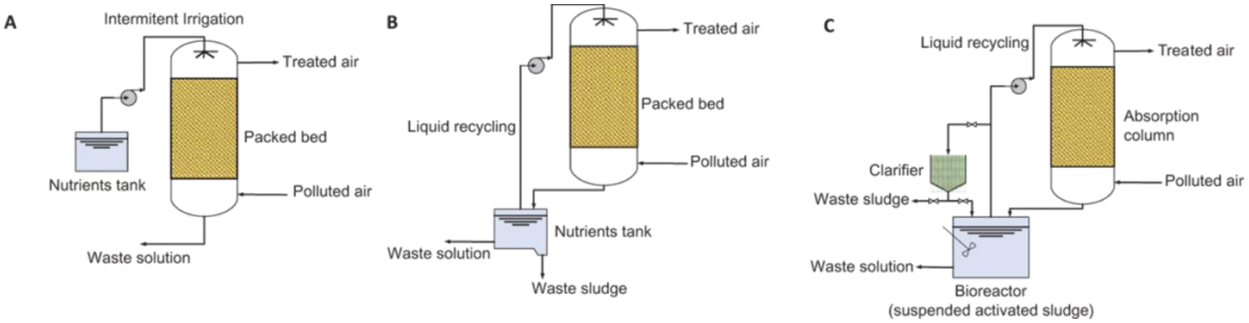

Figure 1 | Schematic representation of a biofilter (A), biotrickling filter (B), and bioscrubber (C) (Muñoz et al., 2015).

Although a lot is known about the microbiome in the rhizosphere, the narrow zone of soil that surrounds plant roots, and their ability of bioremediation, less is known of the above-ground bioremediation, namely phylloremediation (De Kempeneer et al., 2004, Venturi and Keel, 2016). Phylloremediation uses phyllosphere micro-organisms on plants to bioremediate environmental contaminants and has been proposed in literature as a potentially useful approach (Wei et al., 2017).

1.3. Phyllosphere

The phyllosphere is defined as the aerial leaf surfaces of plants and is colonised by a diverse community of micro-organisms, whereby bacteria are by far the most numerous colonists of leaves (Fig. 2) (Lindow and Brandl, 2003). Phyllosphere bacteria are often found in numbers averaging 10^6 to 10^7 cells/cm^2 per leaf. It is estimated that leaves have a surface area of 4 x 10^8 km² across the globe and therefore the global phyllosphere bacterial community consists of as many as 10^{26} cells (Laforest-Lapointe et al., 2017). This represents a major potential source of local microbial organisms to bioremediate air pollutants and to modulate human health.

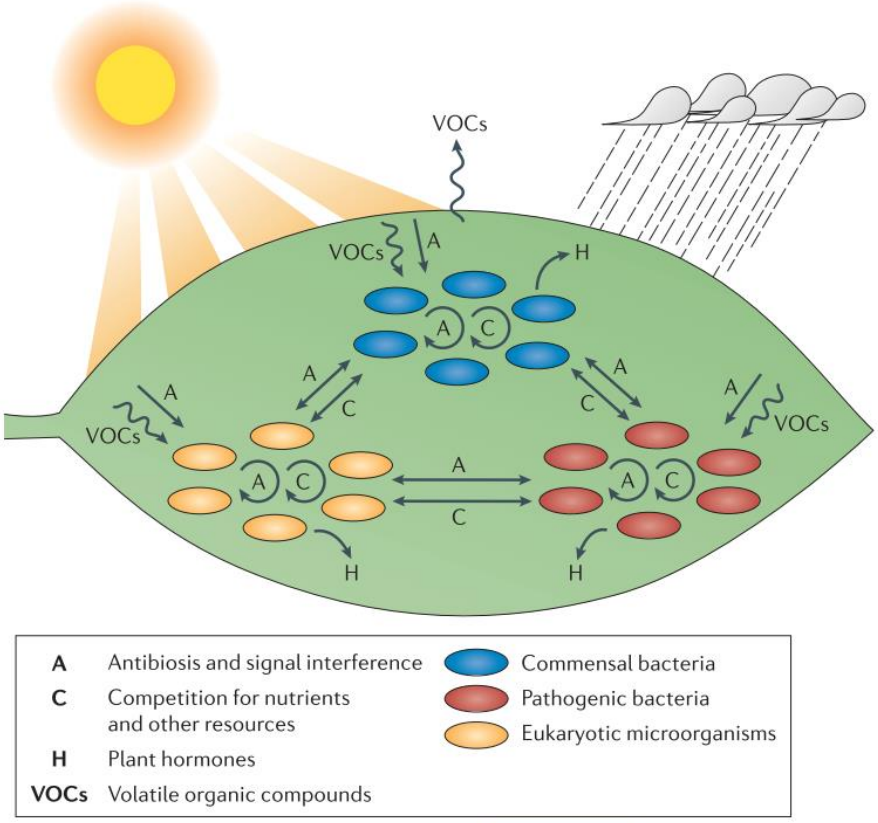

Figure 2 | Interactions expected to occur in the phyllosphere among micro-organisms, between micro-organisms and the plant and between micro-organisms and the environment (Vorholt, 2012). Micro-organisms compete with each other for space and nutrient resources, both within each population and between the populations. Antibiosis, cell signalling and signalling interference systems act among the different groups and also between the plant and the micro-organisms. Micro-organisms might produce plant hormones that affect the plants and plants can produce antimicrobial compounds. In addition, the environmental conditions, including wind, radiation, rain, moisture and, can affect the phyllosphere community. Figure from (Vorholt, 2012)

The phyllosphere is a relatively harsh environment as it provides limited nutrients, is characterized by large fluctuations in radiation and moisture, and contains antimicrobial compounds that are produced by plants or other micro-organisms (De Kempeneer et al., 2004, Vorholt, 2012). The bacterial

composition of the phyllosphere depends on the leaf characteristics, season, climate, geographic location of the host plant, and host plant species (Smets et al., 2016, Wei et al., 2017, Lindow and Brandl, 2003). The latter is illustrated in a study by Redford et al. (2010) whereby the phylogenetic variability of phyllosphere bacteria of 56 different tree species showed a lower variability within a plant species than between different plant species, even over large geographical distances. Similarly, a significant association between tree species and phyllosphere communities has been described for tropical and neotropical trees, trees in temperate forests and Mediterranean perennials (Vokou et al., 2012, Lambais et al., 2006, Kembel et al., 2014, Kim et al., 2012, Laforest-Lapointe et al., 2016). Several studies have shown that leaf bacterial communities differ between urban and rural settings. Many of the dominant non-urban taxa are replaced by other taxa in an urban environment (Smets et al., 2016, Laforest-Lapointe et al., 2017). In addition, bacterial communities differ primarily due to host species identity, responsible for 20% of the variation found by Laforest-Lapointe et al. (2017), urban and rural variation of temperature, humidity (e.g. urban heat islands effect) and atmospheric contamination (Battaglia et al., 2017, Smets et al., 2016).

Phyllosphere bacteria have adapted, among other things, to the nutrient shortage, incident ultraviolet radiation and fluctuating moisture and pH levels in order to survive (Lymperopoulou et al., 2016). The phyllosphere is, in general, suggested to be a carbon-limited environment (Wilson and Lindow, 1994). Therefore, atmospheric particles and pollutants may serve as a nutrient source to many phyllosphere bacteria. In addition, it is suggested that plant-related micro-organisms also strongly influence the composition of airborne bacteria (Lymperopoulou et al., 2016, Fujiyoshi et al., 2017). Despite the extensive knowledge of atmospheric chemistry, the extent of chemical conversions by microbial communities in the air and on the plant surfaces are largely unknown. The ability to bioremediate air pollutants could serve as a novel air cleaning bioremediation technique, namely the application of plant-associated bacteria of the phyllosphere to degrade or remove specific air pollutants from the ambient (indoor) air.

Examples of phyllosphere bacteria including some strains of *Pseudomonas sp.*, *Rhodococcus sp.*, *Alcaligenes sp.*, *Burkholderia sp.*, *Bacillus sp*., and *P. putida* have been found to degrade BTEX (Wongbunmak et al., 2017b, Wei et al., 2017). Other groups of bacteria like cyanobacteria are capable to use a variety of nitrogen sources, like nitrate, nitrite and ammonium (Wei et al., 2017). Besides phyllosphere bacteria, various bacterial biodegradation pathways for the degradation of BTEX and NO_2 have been identified in bacteria.

1.4. Biodegradation pathways of NO_x

The first step of nitrogen oxides transformation and assimilation is cellular uptake, which may occur by passive diffusion or is facilitated by transporters such as NirC, which has been predicted to serve as a bidirectional nitrite-specific transporter. Passive diffusion of NO_2 across membranes may be able in its protonated form (HNO_2, pKa = 3.3) even at neutral pH (Moir and Wood, 2001). In addition, NO and NO_2 can get absorbed and dissolved in the extracellular solution of leaves, whereby they form nitrate (NO_3) and NO_2 in equal amounts (Wei et al., 2017). Nitrate enters the cells via nitrate transporters, such as nitrate/nitrite porter (NNP) and ATP binding cassette (ABC) nitrate transporters. The bacterial NNP is an antiporter whereby they take up nitrate and extrude nitrite. Examples of NNP transporters are NarK and NarU. NarK is highly expressed during anaerobic growth in the presence of nitrate, and plays a central role in nitrate uptake, while NarU has important functions during severe nutrient starvation or slow growth (Fukuda et al., 2015). Periplasmic ABC nitrate transporters are responsible for active nitrate (and nitrite) uptake in these organisms (Moir and Wood, 2001).

After uptake, nitrogen oxides can enter various metabolic pathways. Denitrification, a microbial anaerobic respiration process, is assumed to be the major pathway for NO_3 and NO_2 removal (Chen and Wang, 2015). Hereby, bacteria gradually reduce NO_3 and NO_2 to nitrogen (N_2), via reduction of NO_2 by nitrite reductase to NO, which sequentially is reduced to nitrous oxide (N_2O) and N_2 by nitric oxide reductase and nitrous oxide reductase respectively which are released to the atmosphere (Fig. 3, process 5 and 6) (KEGG, 2019). Recently, many different species have been identified as aerobic denitrifiers, such as *Paracoccus denitrificans*, *Rhodococcus sp.*, and *Comamonas sp.* isolated from sludge, wastewater, and wastewater treatment systems. Ji et al. (2015) proposed that nitrate and oxygen co-respiration in aerobic denitrification is the result of microbial adaptation to allow degradation of toxic nitrogen in relatively harsh environments with reduced carbon-availability and fluctuating oxygen concentrations (Ji et al., 2015). It has to be noted that bacteria found to contain the complete set of enzymes required to carry out each one of the reduction steps that comprise denitrification are scarce (Olivares et al., 2013).

Another process for nitrogen dioxide reduction is *dissimilatory nitrite reduction to ammonium* (DNRA) (Fig. 3, reaction 2), also known as ammonification, which can be linked to the nitrate reduction of NO_3^- (Fig. 3, process 5). In DNRA, ammonium is generated as a result of the anaerobic reduction of NO_2 nitrite reductase (Stein and Klotz, 2016, KEGG, 2019). The resulting ammonium is either assimilated into biomass, such as amino acids or is further oxidized to N_2 via a biochemical process *anammox* (anaerobic ammonium oxidation) using nitric oxide as an electron acceptor (see Fig. 3, process 7) (Stein and Klotz, 2016). Anammox occurs in the anammoxosome, a membrane-bound compartment inside the cytoplasm, of anammox bacteria (e.g., Planctomycetes) (KEGG, 2019). DNRA bacteria are generally found in soils, sediments, anoxic zones in waters characterized by anoxic, electron donor-rich zones with a low nitrate availability (van den Berg et al., 2015).

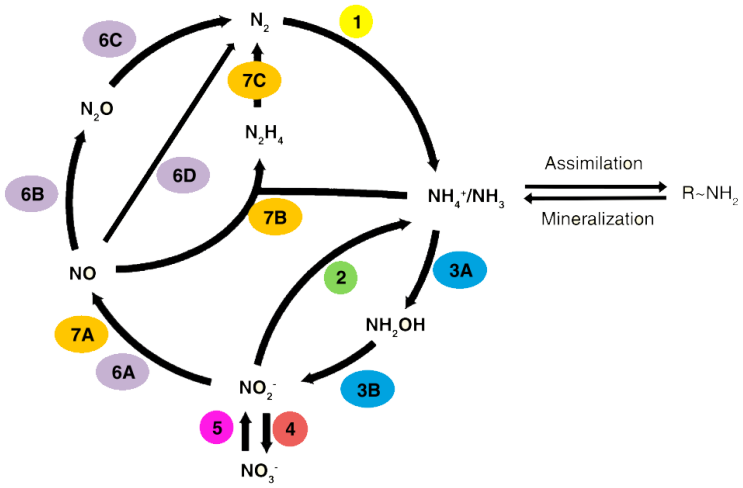

Figure 3 | Major processes of the nitrogen cycle. 1, Ammonification or nitrogen fixation. **2**, Ammonification or DNRA. **3**, nitritation **4**, nitratation **5**, reduction of nitrate to nitrite. **6**, Denitrification or nitrogen-oxide gasification. **7**, anammox or nitrification-denitrification. Figure from Stein and Klotz (2016).

1.5. Biodegradation pathways of BTEX

BTEX are mostly degraded by aerobic pathways as O_2 is a powerful oxidant (Jindrová et al., 2002). The aerobic degradation of BTEX follows different metabolic pathways based on the associated catabolic enzymes present in the micro-organisms (Cao et al., 2009). The enzymes have been divided into upper

pathways, which convert the different aromatic compound to so-called central intermediates, and lower pathways, whereby the enzymes degrade these intermediates further down to molecules that enter the citric acid cycle (Fig. 4) (Cafaro et al., 2004, Ladino-Orjuela et al., 2015). Two aerobic multicomponent enzymatic systems, namely monooxygenases and dioxygenases, have been found in BTEX-degrading organisms to accomplish these pathways (fig. 5) (Jindrová et al., 2002).

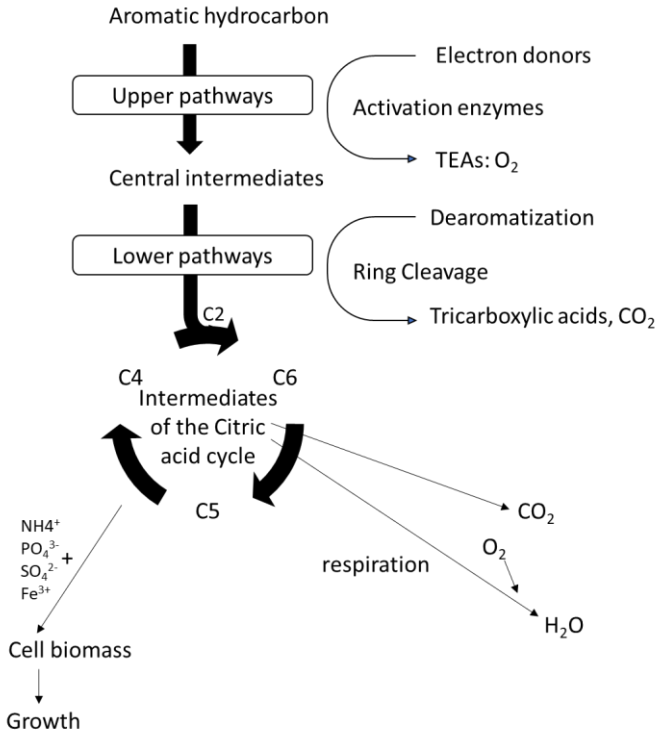

Figure 4 | Schematic representation of the metabolic upper and lower pathways of the aromatic hydrocarbon degradation by bacteria under aerobic conditions. Upper pathways transform hydrocarbon molecules to central intermediates. Lower pathways go from dearomatization of central intermediates to tricarboxylic acids which enter the citric acid cycle to form biomass yield and for respiration. Electron donors: NAD(P)H, $FMNH_2$ or $FADH_2$, ferredoxin, NADH. Activation enzymes: Mooxygenase or dioxygenase enzymes. TEA: Terminal Electron Acceptor. [Adapted from Singh et al. (2017), Ladino-Orjuela et al. (2015)]

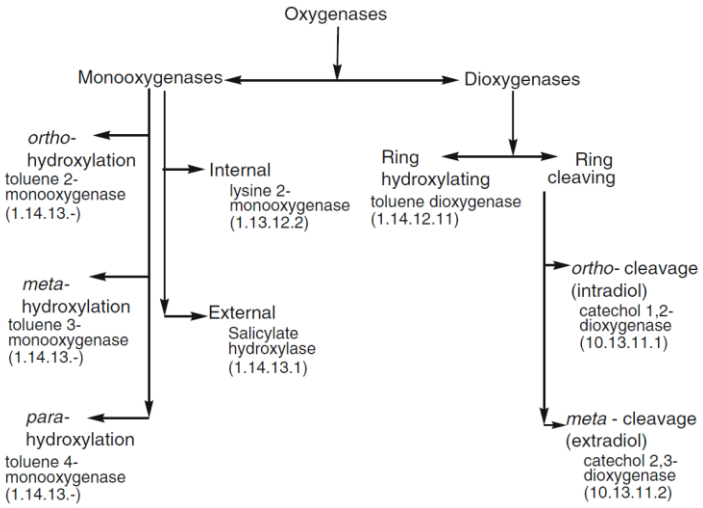

Figure 5 | Classification of oxygenases on the basis of atoms of oxygen incorporated and their position in the aromatic substrate (EC numbers of representative enzymes) (Shrivastava and Phale, 2012)

1.5.1. Upper pathway: oxidation

The upper pathways begin with the oxidation of aromatic compounds and finish with the formation of central intermediates, which can be catechols or non-catecholic compounds. The former have cis-dihydrodiols groups and the latter are hydroxy-substituted aromatic carboxylic acids (Ladino-Orjuela et al., 2015). The upper pathway contains multiple pathways which can be divided into the ring hydroxylation pathways and the alkyl substituent oxidation pathways. In the ring hydroxylation pathway, dioxygenases attack the aromatic rings and generate peroxide intermediates, which are spontaneously transformed in dihydroxyl compounds (e.g. TOD in Fig. 6), while monooxygenases attack the aromatic rings and produce arene oxides as intermediates, which are further converted to phenols (e.g T4MO in Fig. 6). Monooxygenases are capable of performing another monooxygenation on these phenols and convert them to dihydroxyl compounds (Cafaro et al., 2004, Cao et al., 2009, Ladino-Orjuela et al., 2015). In the alkyl substituent oxidation pathways, alkyl substituents are oxidized to produce dihydroxyl compounds (e.g. TOL in Fig. 6)(Cao et al., 2009).

1.5.1.1. Benzene

Benzene can be oxidized by benzene monooxygenases, such as toluene 4-monooxygenase, toluene 3-monooxygenase and toluene ortho-monooxygenase to phenol and catechol by successive hydroxylations. Furthermore, Nitrosomonas aminomonooxygenase of the Nitrosomonas europea ATCC19718 can oxidize benzene to phenol and then to hydroquinone, which can enter the gentisate pathway (Tao et al., 2004, Jindrová et al., 2002).

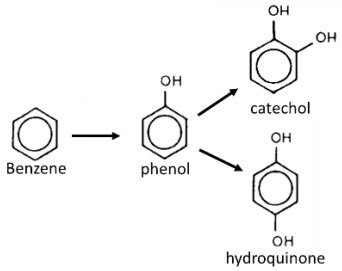

Figure 5 | Metabolic pathway of benzene degradation (upper pathway).

1.5.1.2. Toluene

Toluene can be degraded by many different biodegradative pathways (Fig. 6).

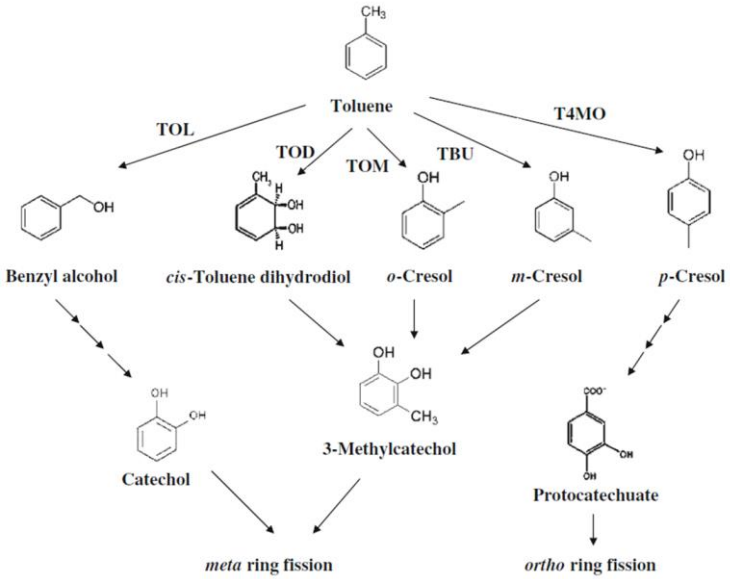

Figure 6 | Five different metabolic pathways of toluene degradation (upper pathway) followed by the ortho- or meta-cleavage by dioxygenases. Toluene side-chain monooxygenase (TOL), Toluene dioxygenase (TOD), toluene o-monooxygenation (TOM), toluene m-monooxygenation (TBU), and toluene p-monooxygenation (T4MO) (Cao et al., 2009).

1.5.1.3. Ethylbenzene

Similarly, many different biodegradative pathways exist for the degradation of ethylbenzene. Naphthalene 1,2-dioxygenase is capable of degrading ethylbenzene to 2-hydroxyacetophenone and/or styrene. The latter can further be oxidized to 3-vinylcatechol. Information concerning the further degradation of 2-hydroxyacetophenone is not known. Ethylbenzene can further be transformed by ethylbenzene dioxygenase to cis-2,3-dihydroxy-2,3-dihydroxybenzene, which can enter a biodegradation pathway with the formation of the central intermediate 2,3-dihydroxy-ethylbenzene (Lee and Gibson, 1996, Jindrová et al., 2002)

1.5.1.4. Xylene

The degradation of xylene is a complex process consisting of multiple oxygenases and dehydrogenase enzymes with intermediates, like m- and p-toluate, in which all xylenes get metabolized to monomethylated catechols, e.g., m-xylene gets metabolized to 3-methylcatechol (KEGG, 2019).

1.5.2. Lower pathway: dearomatization

The lower pathway consists of the dearomatization of the central intermediates which, thereafter, undergo ortho- or meta-cleavage by dioxygenases. In contrary to the upper pathway, the lower pathway enzymes display a significant functional similarity between various bacteria. Hereby, intradiol dioxygenases cleave the ring using the oxygen between the two hydroxyl groups (ortho-cleavage), while extradiol dioxygenases cleave the carbon-carbon bond using oxygen proximal to one of the two hydroxyl groups (meta-cleavage). The resulting products are then entering subsequent pathways leading to the formation of Krebs cycle intermediates, eg. tricarboxylic acids (Cao et al., 2009, Ladino-Orjuela et al., 2015).

1.6. Influences on urban health

1.6.1. Bioaerosols

As phyllosphere bacteria could serve as a novel air cleaning bioremediation technique via the degradation, detoxification and/or assimilation of atmospheric pollutants, they are also considered an important source of bioaerosols (Smets et al., 2016). Bioaerosols are aerosols comprising particles of biological origin or activity (Mirskaya and E. Agranovski, 2018). As discussed above, leaf bacteria form a large fraction of the composition of airborne bacteria. For example, *Sphingomonas* is often found as a bioaerosol in a wide variety of environments due to the frequent abundance on leaves and the apparent high efficiency of plant release (Lymperopoulou et al., 2016). Bioaerosols, originating from phyllosphere bacteria, can furthermore be formed via rainfall, wind-driven aerosolization from dry plants, , dampness or by human activities (Lymperopoulou et al., 2016, Hurst et al., 2007, Mirskaya and E. Agranovski, 2018, Nazaroff, 2016). Vegetation strongly influences the composition of airborne bacteria and the composition of bacteria in indoor air (Lymperopoulou et al., 2016). These outdoor and indoor airborne bacteria and particles can have important effects on human health (e.g. infectious diseases and acute toxic effects) and trigger allergic reactions, leading to more than 224,414 DALY per year in Europe (Jantunen et al., 2011, Bowers et al., 2010). Respiratory symptoms and impairment of lung function are considered the most important health problems caused by bioaerosols, as they are the most widely studied (Kim et al., 2018).

Bioaerosols consisting of phyllosphere bacteria and/or particles can enter the lungs and initiate an immunoreaction by binding to pattern recognition receptors (PRRs). These receptors were originally identified as innate immune sensors that function to distinguish innocuous from pathogenic exposures and induce an appropriate inflammatory response. Extracellular host recognition pathways of gram-negative and gram-positive bacteria occur through PRRs (Tietze et al., 2006). PRRs recognize small molecular ligands conserved within a class of microbes, termed microbe-associated molecular patterns (MAMPs), and endogenous ligands, termed damage-associated molecular patterns (DAMPs) (Bauer et al., 2012). Toll-like receptors (TLRs) is one example of the different types of PRR (Tietze et al., 2006). TLRs are expressed by a wide variety of hematopoietic cells and epithelial cells (West et al., 2006) and can be divided based on their associated specific recognition patterns; Extracellular TLR1, TLR2, TLR4, and TLR5 recognize bacterial components, such as lipoproteins and lipopolysaccharide (LPS) (also known as endotoxin), whereas endosomal TLR3, TLR7, TLR8, and TLR9 recognize nucleic acids (Takeuchi and Akira, 2010).

Interaction of the TLR with its specific ligand is mediated by several extracellular and cell surface host proteins. Proteins involved in LPS recognition include LPS-binding protein (LBP), CD14, MD-2, and Toll-like receptor 4 (TLR4; Hurst et al., 2007). Gram-negative bacteria can release endotoxins, LPS or lipo-oligosaccharides, through membrane fragmentation or blebbing (Hurst et al., 2007). LBP disaggregates soluble LPS, as it is an amphiphilic membrane phospholipid that forms aggregates in aqueous environments, and presents it to CD14. The CD14-endotoxin complex then interacts with MD-2, sending a signal via TLR4 (see Fig. 7). TLR2 is suggested to bind to lipoteichoic acids (LTA), lipoproteins, peptidoglycans, and certain types of LPS, but has the predominant role of recognizing gram-positive bacteria (Martner, 2018). Coreceptors CD36 or CD14 may be involved in the optimal activation of TLR2 (Hurst et al., 2007). After binding, TLRs recruit adaptor proteins such as MyD88 and TRIF, which activate intracellular signalling pathways resulting in the activation of NF-κB (other stimulators for NF- κB are cytokine receptors and TNF receptors), IRFs, or MAP kinases, which regulate the expression of cytokines, chemokines, and type I IFNs (Kawasaki and Kawai, 2014, Kawai and Akira, 2007, Rahman and McFadden, 2011).

Depending on the environment, binding to TLR can lead to different immune reactions (Fig. 8, see appendix) (Lambrecht and Hammad, 2017). In western lifestyle environments, allergies are 20 times more common due to air pollution, lack of physical activity, diet, and spending a high amount of time indoors in well-insulated houses (Lambrecht and Hammad, 2017). In this environment, the binding to TLR2 and TLR4 lead to the up-regulation of proinflammatory cytokines, chemokines, and type1-IFNs such as GM-CSF, IL-33, and thymic stromal lymphopoietin (TSLP). These can boost the capacity of dendritic cells (DCs) to promote T_H2-cell-based immunity by suppressing IL-12 production and upregulating OX40L, resulting in IgE response to allergens. These cytokines can at the same time promote an innate response consisting of basophils, ILC2s, and eosinophils (Lambrecht and Hammad, 2017). On the other hand, in rural environments, the chronic exposure to environmental endotoxins or farm dust can alter the lung epithelial cells, leading to the reduction of the production of IL-33 or GM-CSF, via induction of the ubiquitin-modifying enzyme TNFAIP3. Regulatory lung DCs, that promote the differentiation of allergen-specific regulatory T cells (Treg), are formed under stimulation of chronic exposure to microbial-derived signals or metabolites from the lung microbiome (Lambrecht and Hammad, 2017). Treg cells can probably stimulate the humoral response consisting of IgA and IgG4 responses. In addition, lung DCs promote the allergen-specific T_H1-cell-based immunity, by upregulating IL-12 production as a response to high concentrations of endotoxin (Lambrecht and Hammad, 2017).

The hygiene hypothesis states that the rapid increase of allergies in industrialized countries is a consequence of the lack of early childhood exposure to infectious agents, symbiotic micro-organisms, and parasites leading to an inadequate maturation of the immune systems (Andreae and Nowak-Węgrzyn, 2017, Delli and Lernmark, 2016). One of the most consistent epidemiologic results is the higher prevalence of allergy in urban areas when compared to rural areas (Schroder et al., 2015). For example, there is a significantly lower prevalence of allergic sensitization to harmless environmental particles found in rural children living on farms, or within 5 km of forest or agriculture in comparison to urban children (Mills et al., 2017) Nowadays, more than 30% of children are allergic and more than 10% of children suffer from asthma and allergic rhinitis (Haspeslagh et al., 2018). Lambrecht and Hammad (2017) proposed that barrier tissues such as lung epithelial cells are strongly influenced in a vulnerable period of early life by environment and microbiome diversity and that they have an important role in the immunoregulation in response to allergens. In young children who are at risk of developing allergies, Lambrecht and Hammad (2017) found microbiome dysbiosis in which the overall degree of microbiome diversity was reduced and certain strains were lacking or overrepresented. Colonizing and residential micro-organisms are immune system inducers and pacifiers, capable to positive and negative modulate immune system, altogether adjusting the immune responses to normal levels in healthy humans (Mills et al., 2017). The biodiversity hypotheses identifies a link between biodiversity loss and increase in immune dysregulation in urban populations (von Hertzen et al., 2011). This is illustrated in a study by Lynch et al. (2014), wherein a prospectively and clinical follow-up was performed of children living in inner-city urban neighbourhoods in New York, Baltimore, St. Louis or Boston. Hereby was found that richer and more diverse indoor bacterial communities exposure in the first year of life prevented the development of atopy and recurrent wheeze at age of three (Lynch et al., 2014). Furthermore pet ownership was found to contribute to microbial exposures during infancy and reduce the risk of allergic sensitization (Ownby et al., 2002).

To compensate for the urban effect, Mills et al. (2017) have proposed the Microbiome Rewilding Hypothesis. It states that restoring the biodiverse habitat in urban green spaces can rewild the environmental microbiome to a state that benefits human health, potentially return the co-evolved

ecosystem service of immune protection provided by the microbiomes of natural environments and ultimately leading to decreased immune dysregulation. Rewilding could possibly be achieved by enriching, for example, indoor house plants by spraying phyllosphere bacteria on leaves.

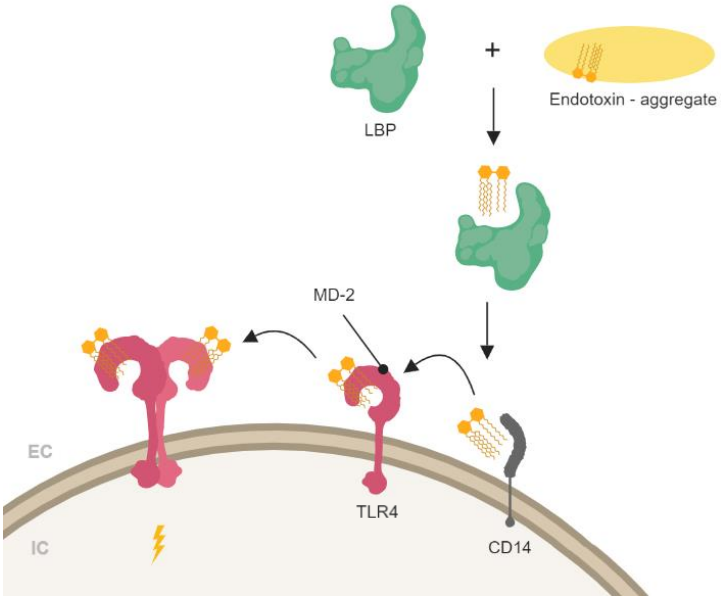

Figure 7. | Extracellular host recognition of endotoxins by Toll-like receptor 4. Endotoxins form aggregates via lipid A. Binding of endotoxins to LBP disaggregates them and endotoxins are then transferred to CD14 as individual molecules. The CD14:endotoxin complex then interacts with MD-2, sending a signal via TLR4 homodimer (created using Biorender), based on the following references

1.6.2. Diesel Exhaust Particles

Particulate matter (PM) is another important contributor to urban atmospheric pollution which is associated with an increased vulnerability to respiratory infections (Chen et al., 2018). Ambient air PM, originating among others form vehicle exhaust emissions, comprises of an elemental carbon core 'soot' to which nitrates, sulfates, semi-volatile or low-volatile organic substances, endotoxins, metals, as well as biological materials are adsorbed (Yang et al., 2017). For 2017, the VMM modelled the concentration of PM2.5 and PM10 in Flanders (Belgium), calculating annual pollutant levels ranging from 19 to 28 µg/m^3 for PM10 and 12 to 17 µg/m^3 for PM2.5 (Fig. 9). The WHO formulated an annual recommended value of 50 µg/m^3 for PM_{10} and 10 µg/m^3 for $PM_{2.5}$ (Vlaamse Milieumaatschapij, 2018). The Antwerp agglomeration and the port of Antwerp were among the highest modulated values found in Flanders (Vlaamse Milieumaatschapij, 2018), ranging from 21 to 30 µg/m^3 for PM_{10} and 12 to 20 µg/m^3 for $PM_{2.5}$. Indoor/outdoor ratios for PM-concentrations were generally greater than one, wherein the presence of indoor sources plays a critical role (Jones et al., 2000, Karakas et al., 2013). Epidemiological studies have indicated a positive association between PM exposure and the increased vulnerability to respiratory infections. However, the underlying mechanisms regarding the effects of PM exposure are lacking and poorly understood (Chen et al., 2018). Many suggested mechanisms have been proposed. PM has been postulated to generate of reactive oxygen species, activate of cell signalling pathways, alter of antioxidant defences, or even suppress the activation of innate defence in response to infection (Paulin and Hansel, 2016, Chen et al., 2018). Due to the highly diverse range

of components varying in chemical composition, phase, and particle size, the cause of these adverse effects are hard to pinpoint (Moretti et al., 2019).

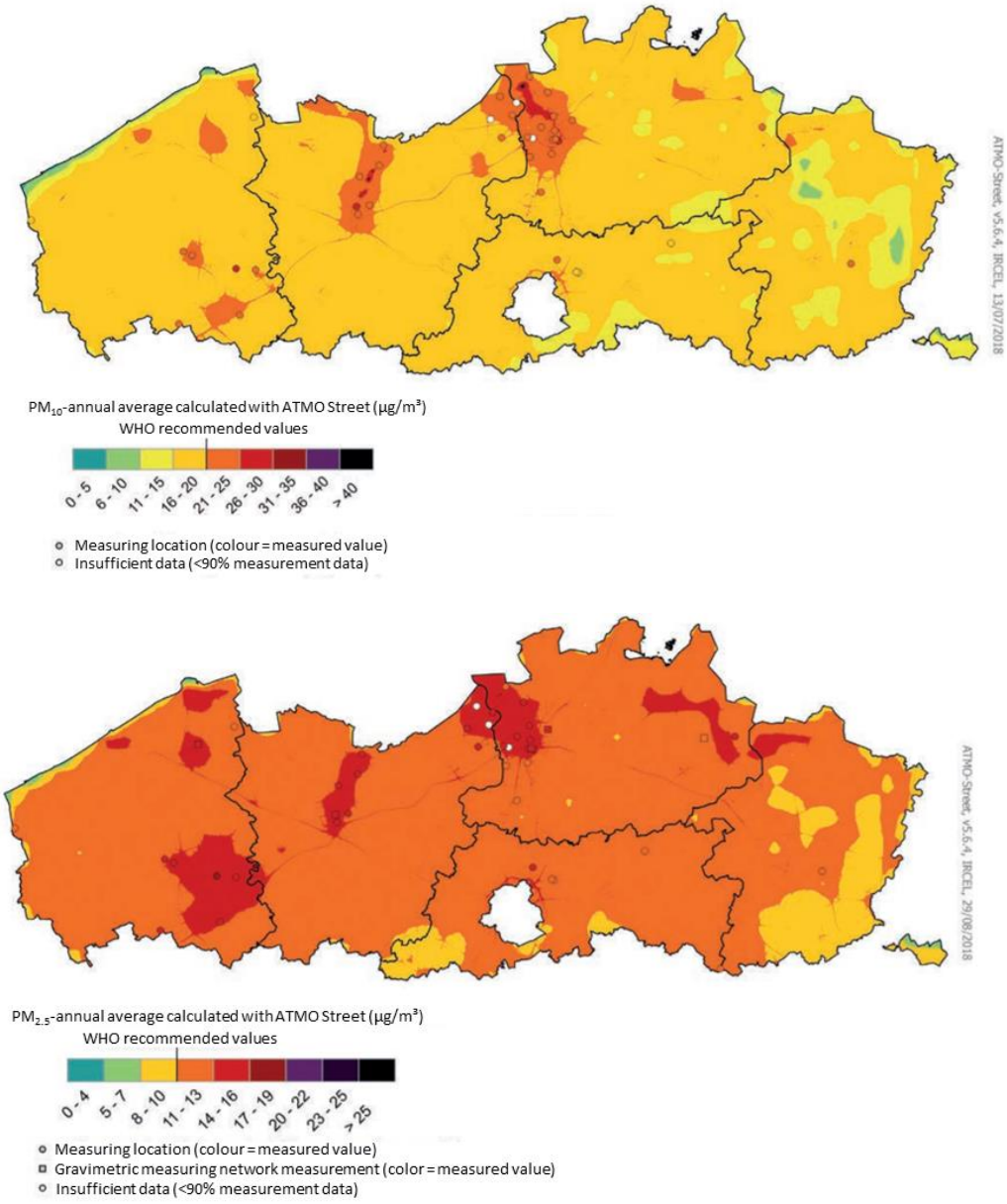

Figure 9. | Modelled PM annual averages in 2017 tested against the WHO annual recommended exposure limit (Vlaamse Milieumaatschapij, 2018).

1.7. Scope of the study

Despite the large surface area of the phyllosphere and their associated microbial communities, little is known of the ability of leaf-associated micro-organisms to bioremediate airborne pollutants or their impact on human respiratory health. The aim of this study was to characterize and quantify the bioremediation capacity of typical indoor urban air pollutants benzene, toluene, ethylbenzene, xylene (BTEX) and NO_x by phyllosphere bacteria isolated during this study and previous studies. Furthermore, the impact of phyllosphere bacteria on the human immune-response was investigated as phyllosphere bacteria are considered an important source of airborne bacterial particles. To this end, modified human THP1 monocyte cells were exposed to bacterial isolates. Bacteria, selected for exposure, were based on the most abundant bacteria in bacterial phyllosphere community of ivy leaves identified by high-throughput 16S rRNA amplicon sequencing, showed a high relative growth rate or which showed active biodegradation BTEX or NO_2. In addition, the immuno-modulating potential of these phyllosphere bacteria on the interaction between diesel exhaust particles (DEP) and modified THP1 cells was investigated.

Chapter 2: Materials and methods

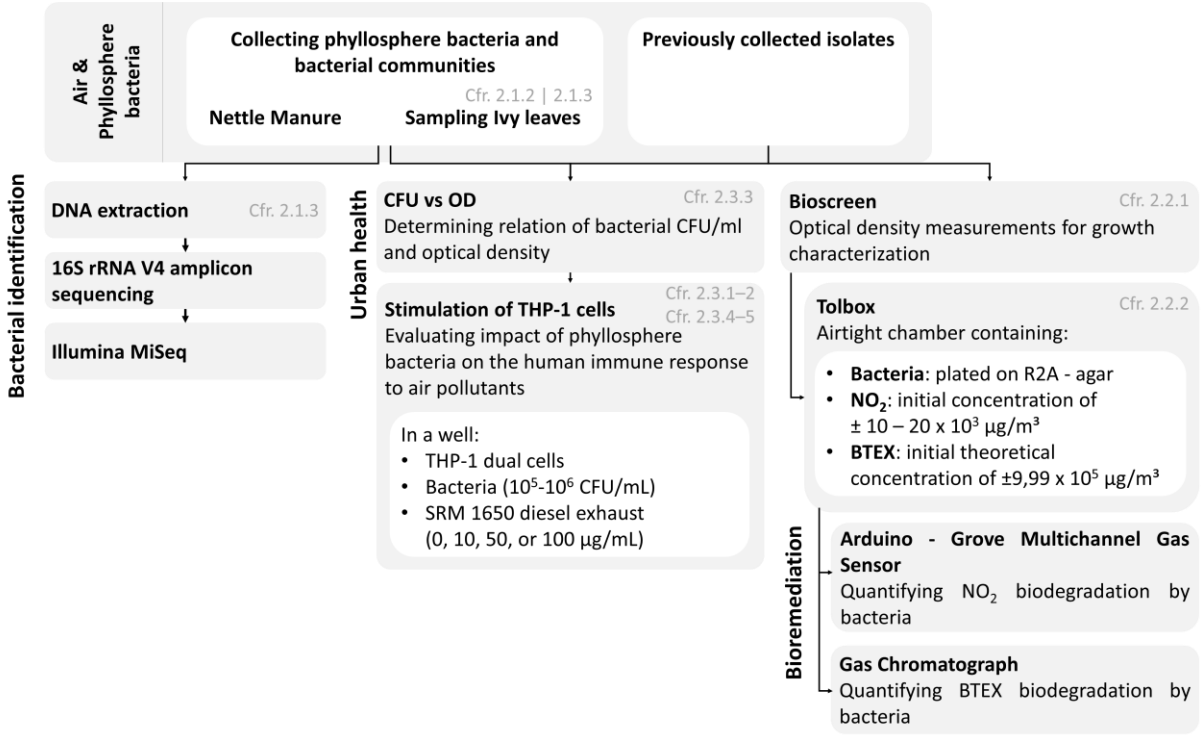

Figure 10. | Overview of the materials and methods and different experiments carried out in this master thesis.

2.1 Preparation and identification of phyllosphere bacteria

2.1.2 Bacterial strains and growth conditions

The phyllosphere bacteria used in this thesis are listed in Table 7. They were isolated in previous studies assessing bacteria of the atmosphere and phyllosphere and were selected for being non-pathogenic to humans or plants. These 34 bacterial strains were added from a pre-existing stock in a volume of 10 mL of Reasoner's 2A (R2A) broth (Lab M) in test tubes. Medium was autoclaved at 121°C for 20 min and cooled to room temperature before inoculation of bacteria. The bacteria were cultured at room temperature until turbid on an orbital shaker and stored in 25% glycerol solution at -80°C for optimal preservation, until further usage.

2.1.3 Bacterial isolation from liquid manure

Additional bacteria were isolated from liquid manure. Liquid manure was made by immersing nettles, which were collected on Campus Groenenenborger (University of Antwerp, Antwerp, 51°10'43.9"N 4°24'59.1"E), in 10L water with an initial temperature of 55°C. Granulated sugar (100g) was added and the nettles were incubated at room temperature. After one week, samples were taken from the surface water and from the water at the bottom of the bin using a plastic pipette. Subsequently, the samples were diluted 10^{-5} in MRS broth (Difco™ Lactobacilli). The diluted samples were plated on MRS agar (70µg/L MRS) containing cycloheximide (100µg/mL) using the streak plate method to isolate pure strains. Plates were incubated at room temperature for a period of 3 to 5 days until colonies were formed. Representative bacterial colonies were selected and subcultured using the streak plate method. Well-isolated colonies were cultured in R2A broth and incubated at room temperature on an orbital shaker. When turbid, a cryostock was made by storing bacteria in a 25% glycerol solution at -80°C. The isolated bacteria were identified using 16S rRNA gene sequencing on the Illumina MiSeq. Hereto, aliquots of 2mL were centrifuged at 10.000g for 2 min and the supernatant was discarded. The pellet was resuspended in 750µL bead buffer (QIAamp PowerFecal DNA Kit, Qiagen), and stored at

-20°C for optimal preservation of DNA until further processing. DNA extraction of the samples was done with the QIAamp PowerFecal DNA Isolation Kit, according to the manufacturer's instructions, except for the last step where DNA was eluted with 60 µL in total. Prior to the DNA extraction, 10 µl spike (*Aliivibrio fischeri*) was added. DNA was also extracted from a falcon tube without leaves, but treated like the other falcons, to identify potential contaminants of the sampling procedure. After DNA isolation, the yields were checked using a Qubit Fluorometer 3.0 (ThermoFisher Scientific). A PCR master mix (MM) was created as shown in Table 2, containing all reagents except for the template DNA and primers. MM was distributed across the reactions wells (16 µl/well) and diluted DNA of each sample, forward and reverse primer, and the control was added to corresponding wells. Subsequently, PCR of the 16s rRNA gene fragment was executed according to the manufacturer instructions (PCR Protocol for Phusion High-Fidelity DNA Polymerase (M0530)). PCR amplification of the 16S rRNA gene was done in 25 cycles using barcoded primers for the V4 region of the 16S rRNA gene as described by Kozich et al. (2013) (Table 2b). Primers with different barcodes (unique sample-specific identifier) were used to attribute the sequences to the original samples via detection of the appropriate barcode after sequencing. The end product of the PCR reaction was checked by determining the presence of DNA fragments of an expected size using agarose gelelectrophoresis. This was achieved by loading 1µl of the resulting amplicons onto a 1 - 1.2% agarose gel together with 10µl loading dye and 4µl of water. The setup ran for 50 min at 60V. The GeneRuler Express DNA ladder (Thermo Scientific) was used for estimation of the size of the DNA strands. If the PCR was successful, the resulting amplicons were purified using Ampure XP (Agencourt) with a magnetic block, according to manufacturer instructions, and DNA concentration of every well was quantified using the Qubit fluorometer 3.0. Based on these DNA concentrations, samples were pooled at equimolar concentrations into one tube. The pooled amplicons (diluted to 2nM) were sequenced at the Centre for Medical Genetics (Edegem, Belgium) with Illumina MiSeq, using the 500-cycles MiSeq Reagent Kit v2 (Illumina). The EzBioCloud 16S rRNA gene database, downloaded on 08/01/2018, was used as reference database (Yoon et al., 2017). The resulting bacteria were compared between urban and non-urban on abundance. The most abundant, which can be cultivated, were selected for further experiments.

Reaction mixture	**1x**	**7x + 10%**
Molecular grade water	10.8	83.16
dNTPs (10 mM)	0.4	3.08
5x MM Phusion HF buffer	4	30.8
DMSO	0.6	4.62
Phusion DNA polymerase	0.2	1.54

PCR procedure			
Steps	Temperature	Time	
Denaturation	95°C	2 min	
	95°C	20 s	25 cycles
Annealing	55°C	15 s	
Extension	72°C	1 min	
Final extension	72°C	10 min	
hold	10°C		

Table. 2 | Left: Composition of MM used for one PCR reaction. Volumes are given in µl. Right: Reaction steps during PCR amplification.

2.1.4 Phyllosphere sampling (Ivy), DNA extraction and 16S rRNA V4 amplicon sequencing

The composition of bacterial communities of ivy leaves was investigated via Illumina sequencing to get an indication for selecting bacteria in further experiments. Hereto, ivy leaves were collected at 1 to 2 meters above the ground at three different urban locations in the city of Antwerp and at three non-urban locations in more rural areas surrounding the city. The non-urban collection sites were located at the edge of the Kalmthoutse Heide, a protected nature reserve (location 1 and 2, Fig. 11), and in the centre of the protected forest Zevenbergenbos (location 3, Fig. 11). The urban locations (locations 4

to 6, Fig. 11) were selected in densely built areas close to busy roads. The mean atmospheric concentrations of NOx, measured in the period of 28 April 2018 to 26 May 2018 by Curieuzeneuzen (Meysman and De Craemer, 2018) and the estimated annual mean (2017) of PM_{10}, $PM_{2.5}$, and black carbon, modelled by the Vlaamse Milieumaatschapij (www.vmm.be) are shown in Table 3 and were consistently lower at the non-urban locations compared to the urban locations. The sampling took place at an air temperature of 10 to 13°C over a period of 3 hours without any rain. Per location, 4 healthy, vegetative, and undamaged leaves were collected from *Hedera sp*. (*H. helix* or *H. hibernica*; common name: ivy) plants. This was achieved by cutting the leaves on the border of the leaf and the petiole and putting them in a 50 mL falcon tube, which was transported on ice. Upon arrival in the lab, the leaves were washed with 5 mL leaf-wash-buffer (Redford and Fierer, 2009). To suspend the bacteria in the buffer, the tubes were vortexed at max. speed for 5 minutes with the Vortex Genie® 2 (MoBio). Thereafter, the falcon tubes were centrifuged up to 400g for 5 minutes to allow the leaves to be removed. Subsequently, the surface area of the removed leaves was measured by means of a leaf area meter (LI-3100C, LI-COR). The bacterial community composition was determined using 16S rRNA gene sequencing on the Illumina MiSeq as described above.

2.1.5 PM10 quantification via magnetic analysis

During the sampling, another six leaves were collected per location to determine the pollution of particulate matter (PM) on the ivy leaves. Leaves can act as natural accumulators of atmospheric pollutants and the bio-magnetic properties of PM in the leaves allow to estimate local PM pollution (Kardel et al., 2011). The collected leaves were stored in a paper envelope and on the same day as the sampling, the surface area of the fresh leaves was measured by means of a leaf area meter (LI-3100C, LI-COR). Then, the leaves were oven-dried at 45°C for 4 days. Following the protocol described by (Kardel et al., 2011), the dried leaves were tightly packed together in pairs in plastic foil, to avoid moving of the leaves and pressed into a 6.7 cm^2 plastic container. The leaves were magnetised in a pulse DC magnetic field of 1 Tesla using a Pulse Magnetizer (Molspin Ltd) and the saturation isothermal remanent magnetisation (SIRM) was measured immediately using a JR-6 Spinner Magnetometer (Agico). Calibration of the magnetometer with the JR CYS26 calibration standard and measurements of the samples were performed according to manufacturer instructions. The measured magnetic signals (A/m) were normalized by, leaf area (m^2) and volume of the plastic containers (m^3). Each SIRM value was the average of two measurements on the same sample.

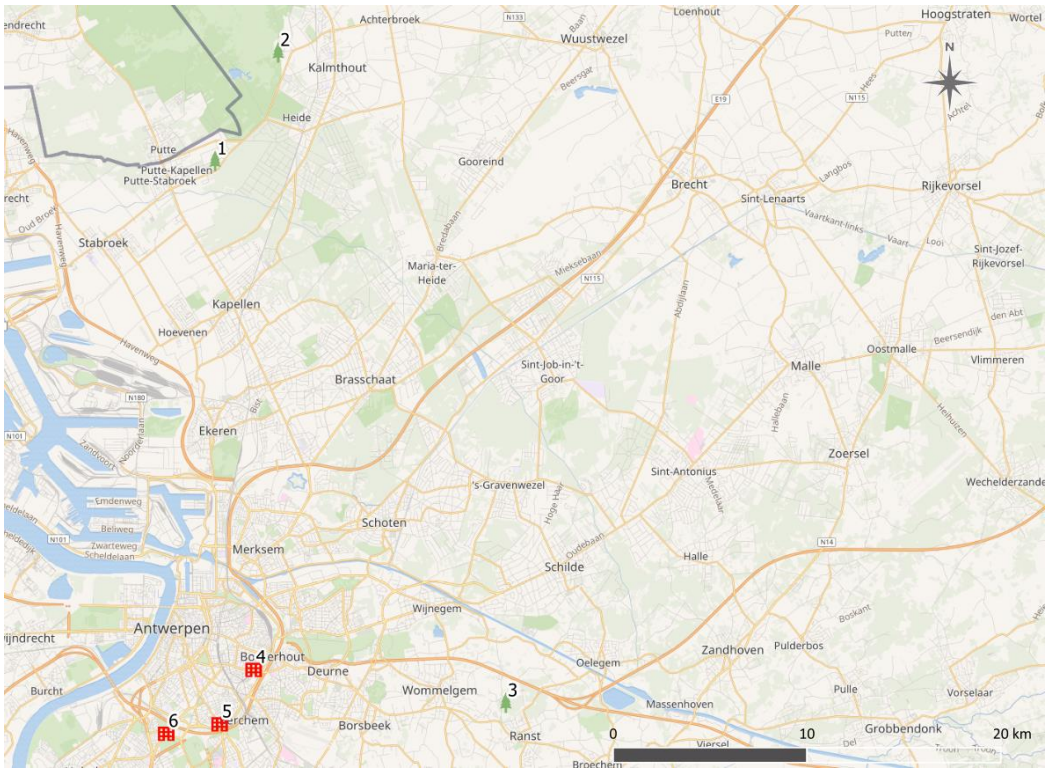

Figure 11. | Sample locations in the province of Antwerp. Non-urban location indicated in green: (1) Korte Heuvelstraat, Kalmthout (51°23'14,7"N 4°26'56,1"E); (2) Vierhoevenstraat, Kapellen (51°21'21.8"N 4°25'10.7"E); (3) Zevenbergenbos, Ranst (51°11'56,7"N 4°33'15,9"E). Urban location indicated in red: (4) Plantin en Moretuslei, Borgerhout (°12'31,5"N 4°26'15,5"E); (5) Grote Steenweg, Berchem (51°11'34,6"N 4°25'18,8"E); (6) Jan van Rijswijcklaan, Antwerpen (51°11'24,8"N 4°23'49,7"E). Map created using QGIS.

Location	coordinates	municipality	Land use	NOx (µg/m³)	PM_{10} (µg/m³)	$PM_{2,5}$ (µg/m³)	Black carbon (µg/m³)
1	51.356064 N, 4.419640 E	Kapellen	Non-urban	15-20	16-20	11-12	0,51-1,00
2	51.387427 N, 4.448910 E	Kalmthout	Non-urban	15-20	16-20	11-12	0,51-1,00
3	51.199092 N, 4.554420 E	Ranst	Non-urban	20-25	16-20	11-12	0,51-1,00
4	51.208759 N, 4.437652 E	Borgerhout	Urban	40-45	21-25	13-15	2,01-2,50
5	51.192955 N, 4.421895 E	Berchem	Urban	40-45	26-30	16-20	2,51-3,00
6	51.190219 N, 4.397139 E	Antwerp	Urban	40-45	21-25	13-15	1,76-2,00

Table 3. | Location-specific atmospheric concentrations of NOx, PM_{10}, $PM_{2,5}$, and black carbon on the sample location in the province of Antwerp (Meysman and De Craemer, 2018, Vlaamse Milieumaatschapij, 2018).

2.2 Biodegradation

2.2.1 Bioscreen

The growth phases of the bacterial strains in R2A broth were determined over time via a bioscreen assay in order to standardize the measurement of the bioremediation capacity of bacteria. By measuring the turbidity of the liquid culture over time, an optical density (OD) curve was generated,

which reflects the growth of the tested bacteria. Hereto, 34 phyllosphere bacteria were cultured in R2A broth and incubated at room temperature on an orbital shaker. When turbid, bacteria were added in triplicate to a 96-well microplate (VWR). Each well contained 20 µl culture and 180 µl R2A-broth medium, with the exception of the wells at the border of the microplate, which contained 180µL R2A-broth medium to reduce edge effect. Optical density (OD) measurements were performed by Synergy™ HTX Multi-Mode Microplate Reader (Biotek). For 2 days, measurements were done at 600 nm (OD600), every 20 minutes, preceded by 10 s shaking.

2.2.2 Bioremediation measurement by GC-FID and MGS

Phyllosphere bacteria were screened on their bioremediation capacity in the presence of pollutants. Bioremediation capacity was standardized on the basis of the growth chart generated with the bioscreen. Standardization was achieved by culturing bacteria from the broth onto agar based on the measured OD complementary to the exponential growth phase. The OD was measured by pipetting 800µl broth in a 1 mL plastic cuvettes and measuring the absorption at 600nm (OD600) using a BioPhotometer plus spectrophotometer (Eppendorf). Depending on the growth chart, 150µl of turbid bacteria-containing-broth was added onto an R2A-agar plate to create a confluent bacterial lawn. In order to facilitate the diffusion of gas throughout the petri dish, a few incisions were burned in the side of the Petri dishes using an inoculation loop. The plates were incubated in an anaerobic jar (3L; Schuett-Biotec GmbH) for 1–4 days at room temperature. During incubation, the bacteria were acclimatized to the pollutants by culturing them in the presence of a 3µl BTEX-mixture, containing benzene, toluene, ethylbenzene and o-xylene at a volume of 0,6 µl each and p- and m-xylene at a volume of 0,3 µl each. Prior to placing the plates in the Tolbox, the plates were removed from the anaerobic jar to desaturate for one hour.

Batch experiments were conducted to quantify the bioremediation of toluene, benzene, ethylbenzene, xylene, and nitrogen dioxide using the Tolbox (Fig. 12). The Tolbox is an optimized, modular, airtight chamber that acts as a bioreactor. The Tolbox is equipped with ventilator (OD8038 VXC, Orion Fans) inside to create a homogenous distribution of the air. Quantitive degradation of the air pollutants BTEX by the bacteria that are incubated inside was followed in real-time by gas chromatography (GC) flame ionization detector (CompactGC 4.0 from Global Analyzer Solutions). The capillary column was kept isothermal at a temperature of 60°C. The injection temperature was 50°C and the FID temperature was 150°C. Helium was used as carrier gas at a stable flow rate of 20 mL/min. The combustion gas flow-rates of air and helium were set at 350 and 35 mL/min, respectively. Chromeleon v7.0 (ThermoFisher Scientific) was used as a laboratory data management system. Bioremediation of NO_2 was quantified using a Multichannel Gas Sensor (Seeed Studio) connected to an Arduino Uno REV3 (Arduino). Arduino IDE (Arduino) was used as a laboratory data management system. Selected bacterial isolates were compared to a positive bacterial control Methylibium petroleiphilum (LMG 22953), known to bioremediate toluene, benzene, and ethylbenzene in mineral salt medium (Nakatsu et al., 2006b, Hristova et al., 2007). Blank plates in which no bacteria were added were tested to account for BTEX loss due to adsorption and factors other than biodegradation by the phyllosphere bacteria, such as atmospheric oxidation (Thompson et al., 2003). In each run, six plates of a bacterial strain grown on agar were exposed to a mixture of TEX and NO_2. Liquid toluene and ethylbenzene were added in a volume of 7µl each to the Tolbox (Volume of 61L) and the isomers O-, P-, and M-xylene were added respectively in a volume of 7µl, 3,5µl and 3,5µl. When active biodegradation was measured, the experiment was repeated and benzene was added to the mixture at a volume of 7µl. After evaporation, each BTEX had an initial theoretical concentration of ±9.99 x 10^5 µg/m³ in the

Tolbox. NO was injected from a compressed gas cylinder into the tolbox for one minute at a flow rate of 50mL/min together with N_2 as carrier gas at a flow rate of 500mL/min. The concentration was measured over a period ranging from 24 h to 48h (±400 measurements/24h).

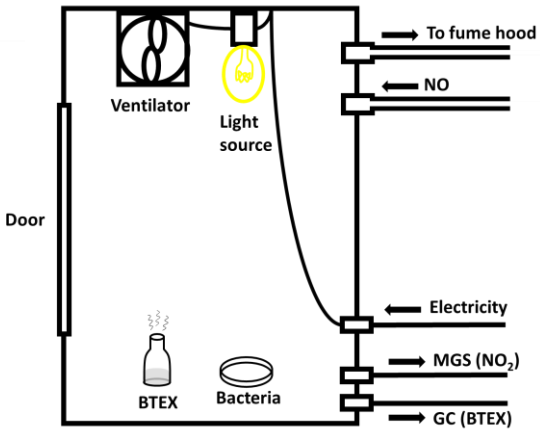

Figure 12 | Schematic overview of the Tolbox. The Tolbox is an airtight chamber, equipped with a ventilator to create a homogenous distribution of the air. The tolbox is connected to a gas chromatograph (GC) and a multichannel gas sensor (MGS) to quantify the degradation of air pollutants BTEX and NO_2 respectively by the bacteria that are incubated inside. BTEX was added in liquid form which evaporates and NO injected into the tolbox from a pressurized cylinder.
GC, Gas Chromatograph; MGS, Multichannel Gas Sensor.

2.3 Urban health

The immuno-stimulating potential of bacteria, described in Table 1 and obtained via nettle manure isolation (see above cfr 2.1.2), were tested using THP1-Dual™ cells (InvivoGen) and diesel particulate matter SRM1650B.

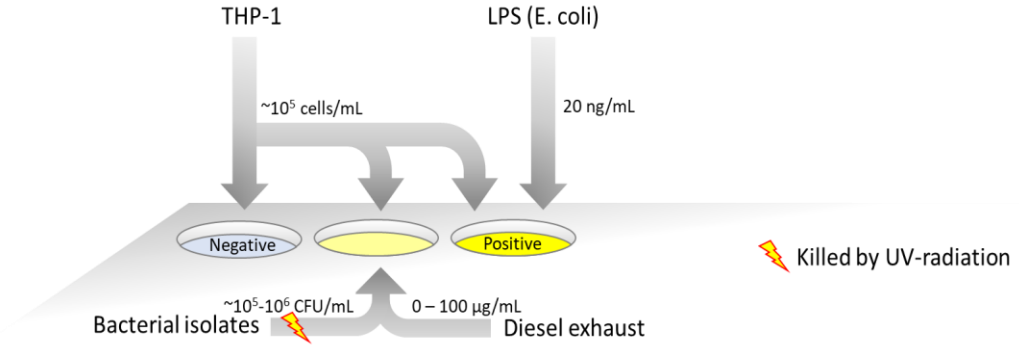

Figure 13 | Overview of the experimental setup. Negative control consisted of THP1 Dual cells with LPS-free medium. Positive control was created by combining THP1-Dual cells with LPS. Immune-inducing and modulating potential was tested by exposing THP1-Dual cells to bacterial strains (10^5-10^6 CFU/mL), killed via UV-radiation, and varying concentrations of DEP (0, 10, 50, or 100 µg/mL).

2.3.1 Preparation of the diesel exhaust particles

The immunomodulating potential of phyllosphere bacteria on the interaction of diesel exhaust particles and human monocyte THP1-Dual cells was determined by exposing THP1 cells to the selected

bacteria in combination with standard reference material (SRM)-1650b. SRM-1650b is diesel exhaust particulate material (DEP) collected from heat exchangers of four-cycle heavy-duty diesel engines operating under a variety of conditions. The average particle size of SRM-1650B was 0.18µm and the surface composition of polycyclic aromatic hydrocarbon is listed in Table 8 and 9 (NIST, 2013). The adsorbed metal and endotoxin composition to the surface of SRM-1650b was determined by Gurpreet (2013) and consisted of sodium (<1% w/w), phosphorus (<1% w/w), Zinc (<1% w/w), Nickel (<1% w/w), and boron (~2% w/w). No endotoxin content was found on DEP (Gurpreet, 2013). SRM-1650b was dissolved in PBS at a stock concentration of 0.666 mg/mL. The SRM-1650b solution was then sonicated for 2 min in a water bath to disaggregate particles, aliquoted into 2 mL Eppendorf tubes, and stored at -20°C until further use.
Prior to treatment of THP1-Dual cells, SRM-1650b was again sonicated for 2 min and diluted in R2A broth to give a concentration of 10, 50, or 100 µg/mL Concentration was chosen based on the findings by Gurpreet (2013): monocyte-derived macrophages (MDM) exposed to 10 to 100 µg showed no reduction in cell viability. However, MDM from COPD patients exposed to 300µg/mL SRM-1650B resulted in a significant reduction of viability of ± 35% (Gurpreet, 2013).

2.3.2 Preparation of the phyllosphere bacteria

To investigate the immune-inducing potential of phyllosphere bacteria in THP1-Dual cells, bacterial cultures were diluted to a concentration of 10^5 and 10^6 colony forming units/mL (CFU/mL). Prior to the preparation of phyllosphere bacteria, the CFU/mL in function of the OD was determined for each bacterial isolate, which is described in cfr 2.3.4. Based on the CFU/mL, the bacteria were resuspended to a concentration of 2 x 10^5 and 2 x 10^6 CFU/mL in fresh RPMI-medium, containing no Pen-strep (Gibco). A small volume was taken from the 10^5 dilution to re-confirm the CFU / mL. The remaining bacteria were killed by UV-irradiating them twice for 15 minutes using the built-in UV-lamp of the biosafety cabinet (Telstar) and vortexing them in between. To confirm, a viability test was performed by plating the bacteria onto R2A-agar and look for growth.

2.3.3 Calculation of CFU/mL

Colony-forming units is used to measure the microbial load. In order to calculate the CFU/mL, bacterial isolates were inoculated into a test tube containing 10 mL R2A broth and incubated at room temperature on an orbital shaker. When the medium was turbid, the OD600 was measured using a BioPhotometer plus spectrophotometer (Eppendorf). Subsequentially, a serial dilution series was made in triplicate (10^0 – 10^{-7}) using sterile R2A broth. R2A agar was used for all plate media. Immediately after dilution, 15 µl of each dilution were transferred to a plate using the drop plate technique, as described by (Herigstad et al., 2001). Drop plating was performed using an electronic pipetter. Each agar plate was divided into four quadrants, each quadrant reserved for one dilution in the series. The plates were incubated on room temperature until colonies could be counted. The CFU/mL was calculated using the following formula:

$$CFU/mL = \frac{no.of\ colonies * dilution\ factor}{volume\ plated}.$$

The CFU/mL is equal to the average number of colonies counted in the transferred drop, corrected by the dilution factor of the countable dilution and the volume of the drop that has been transferred to the plate.

2.3.4 Thawing and maintaining THP1-Dual cells

THP1-Dual™ cells are NF-kB-SEAP and IRF-Lucia luciferase Reporter Monocytes that were derived from human THP1 monocyte cell line. This immortalized monocyte-like cell line was isolated from the peripheral blood of a 1-year old male patient with acute monocytic leukaemia (Chanput et al., 2014).

When stimulated, THP1 cells adhere to culture plates accompanied by differentiation into a macrophage phenotype (Qin, 2012). In THP1-Dual cells, *Secreted embryonic alkaline phosphatase* (SEAP) is transcribed when the NF-kB pathway is induced and secreted luciferase (Lucia) is produced after induction of the IRF pathway. During this thesis, the induction of NF-kB in THP1-Dual cells by bacteria and diesel particulate matter was only studied using the SEAP reporter which was visualized by adding a substrate para-Nitrophenylphosphate (pNPP). PNPP turns yellow after metabolization by the produced SEAP and was quantified at an OD of 405.

THP1-Dual cells were stored in liquid nitrogen according to the instructions of the manufacturer. In preparation for the exposure experiment, THP1-Dual cells were removed from the liquid nitrogen and quickly thawed at 45.1°C in a bead bath (Memmert). Subsequently, the cells were washed in 15mL RPMI1640 (Gibco) containing 20% heat-inactivated FCS (GE Healthcare) and 25 mM HEPES (ThermoFisher Scientific). After spinning down at 300 g for 5 minutes and discarding the supernatants, the cells were resuspended in RPMI (20% FCS, 25 mM HEPES) and incubated in a T25 flask at 37°C, 5% CO_2 for 1 to 3 days. The THP1-Dual cells were passaged every 3 days to prevent the concentration to exceed 2 x 10^6 cells/mL, by inoculating 5 x 10^5 cells/mL into a new flask. This was achieved by transferring the medium from the flask to a 50 mL falcon, spinning down the cells at 300 g for 5 minutes using the centrifuge 5702 (Eppendorf), discarding the supernatants and resuspending the cells in three times the volume used in the original flask. Subsequently, the cells were counted using the EVE automatic cell counter (Nanotek), according to the instructions of the manufacturer. The concentration was adjusted to 5 x 10^5 and the cells were split by transferring 15 mL into new T75 flasks. During the second passage, 50 mg/mL Normocin (Invivogen) and 10000 U/mL Pen-strep (Gibco) were supplemented to the growth medium to keep the cells free of microbial contaminants. To maintain selection pressure, 10mg/mL blasticidin (Invivogen) and 100mg/mL Zeocin (Invivogen) were added to the culture medium every other passage. These selective antibiotics served to maintain the plasmids in the cell line. The growth conditions are visualized in Table 4.

Growth medium	Concentration	Passage						
RPMI1640		Revival	First passage	Second passage	Third passage	Fourth passage	…	…
Heat-inactivated FCS	10 % (20 % - Revival)							
HEPES								
Normocin	50mg/mL							
Pen Strep	10,000 U/mL							
Blasticidin	10mg/mL							
Zeocin	100 mg/mL							

Table 4. | Growth media constitution based on the passage. THP1-Dual cells were revived in growth medium containing RMPI1640, FCS, and HEPES. Afterwards, cells were passaged to a new 75 cm² flask containing additional normocin and Pen strep. Blasticidin and zeocin were added to the growth medium every other passage starting from the second passage.

2.3.5 Stimulation of THP1- Dual cells

Prior to the experiment, the THP1-Dual cells were transferred from the T75 flask to a falcon tube and spun down at 300 g for 5 minutes. The cells were resuspended in growth medium containing RPMI1640, 10% FCS, HEPES, and 20,000 U/mL Pen strep and were counted using the EVE automatic cell counter (Nanotek). Based on the cell count, the concentration was adjusted to a concentration of 0.25 to 0.5 x 10^6 cells/mL. Thereafter, 100 µl of cell suspension was added to each well of a flat-bottom 96-well plate. Afterwards, the THP1-Dual cells were treated with phyllosphere bacteria, added at a volume of 100 µl, and increasing concentrations of SRM-1650B (Table 5). SRM1650b solution (0,666 mg/ml) was added at volumes of 0, 3, 15, and 30µl to the cell suspension to create concentration of 0,

10, 50, and 100µg/mL respectivily. Preparation of phyllosphere bacteria and SRM1650 is discussed above (cfr. 2.3.1 and 2.3.2 respectively). The positive control was created by adding 100µl of LPS solution (20ng/mL) to 100µl THP1-Dual cells. LPS was from E. coli (Sigma). The negative control was created by supplementing 100 mL of endotoxin-free RPMI medium to the THP1-Dual cells. The plate was incubated at 37°C, 5% CO_2 for 20 to 24 h.
After incubation, the cells were checked on viability, cell morphology, and bacterial/fungal growth. Subsequently, 50 µL of the supernatant was transferred to corresponding wells of a new plate. To detect the SEAP production, 100 µl of pNPP (1,5mg/mL) solution containing 1 M Tris HCl, 1M NaCl, and 50 mM $MgCl_2$, was added to each well and thereafter covered with aluminium foil. After 20 minutes of incubation at room temperature, the absorbance was measured at an OD of 405 nm with the Synergy HTX Plate Reader (BioTek). This experiment was repeated and the results were compared among each other.

					Test solution							
	Volume	**Final concentrations**	-	+	a	b	c	d	e	f	g	h
THP1-Dual cells	100µl	10^5 cells/mL										
Bacterial cultures	100µl	10^5-10^6 CFU/mL										
LPS-free RPMI medium	100µl											
LPS-solution	100µl	20 ng/mL										
SRM1650	0µl	0 µg/mL										
	3µl	10µg/mL										
	15µl	50µg/mL										
	30µl	100µg/mL										

Table 5 | overview of the combination tested during THP1-Dual cell exposure experiment. Grey boxes depict the solutions which were combined per testing condition. The negative control was created by combining THP1-Dual cells and LPS-free RPMI medium. Positive control was created by combining THP1-Dual cells and LPS-solution. Positive control and negative control are indicated by "+" and "-" respectivily. A to g show the different combinations to evaluate the influence of bacteria and DEP on THP1-Dual cells.

2.4 Data analysis

Statistical analyses were done in R-studio (R Core Team, 2018). A significance level of 0.05 was used for all statistical tests. The graphics and the tables were expressed as mean ± standard error of the mean (SEM).
The 16s illumina data was analysed and manipulated using the DADA2 package (Callahan, 2019) and the Tidyalmplicons package (Wittouck, 2019). A Bray-Curtis dissimilarity matrix of the sequence data was calculated, using the tidyamplicon package (Wittouck, 2019). Nonmetric multidimensional scaling (NMDS) was applied to this Bray-Curtis dissimilarity matrix to visualize the data in two dimensions. SIRM data per plant was measured by taking the mean of the three SIRM values and performing a natural logarithmic transformation to obtain normally-distributed data. The transformed SIRM values of urban and non-urban plants were compared using a unifactorial analysis of variance (ANOVA) and Tukey's test.

Bioscreen growth curves were analysed using R script BAT2.0 developed by Thulin (2018).
Bacterial bioremediation of the pollutants in the tolbox were expressed as a percentage efficiency of the removal of BTEX, using the following equation:

$$\frac{C_O - C_F}{C_O} * 100\%.$$

C_0 is the concentration (area under curve) after the initial drop and C_F is the final concentration (area under curve) at 24 h and 48 h (fig 14). By excluding the measurements before C_0, the uptake of pollutants by the agar, Tolbox walls, and other plastics (plates, ventilator) were avoided. Degradation capacity was compared to the percentage efficiency of blank plates.

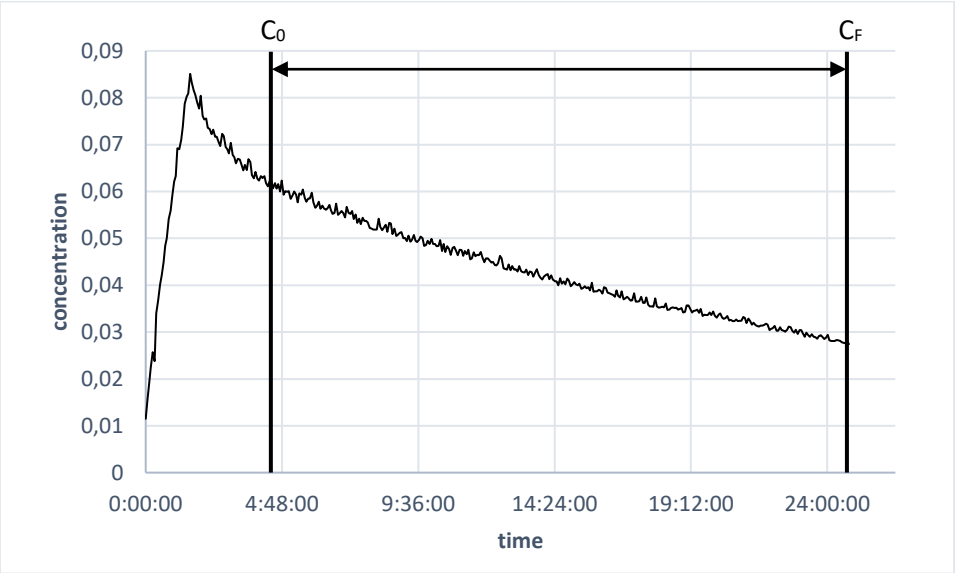

Figure 14 | Ambient pollutant concentration over time measured in the Tolbox. Analysis will be performed on the marked section. The increase in concentration before the peak concentration is due to evaporation of the pollutant. The fast decrease between the peak and the marked section is probably due to uptake of pollutants by the agar, Tolbox walls, and other plastics (plates, ventilator).

The statistical analysis of the inter-group differences of the reporters of the immune reaction among the bacterial strains and among the different concentrations of diesel exhaust particles was compared using unifactorial ANOVA and Tukey's test. The interaction between bacterial isolates and the different concentration of SRM-1650b were tested using multifactorial ANOVA.
Normal distribution of data was verified using the Shapiro-Wilk test. In cases when the data did not meet the assumed conditions of the analysis of variance, data were subjected to logarithmic transformation or non-parametric analytical equivalent Kruskal-Wallis test and Dunn's test.

Chapter 3: Results

3.1 Sampling phyllosphere communities

Ivy leaves were sampled to identify abundant phyllosphere bacteria (Cfr 3.1.2) for the selection for further experiments. Additional bacteria were isolated from Liquid manure form nettle manure as described below (Cfr. 3.1.3).

3.1.1 Higher Leaf SIRM in urban locations

Ivy leaves were collected at 6 different locations in the province of Antwerp. To estimate the traffic-generated PM, a magnetic analysis was performed (Fig. 15). Leaf SIRM was significantly affected by the sample location. The non-urban leaf SIRM values, with an average of 81.9 ± 20.00 mA, were significantly lower than the urban leaf SIRM (average of 339.0 ± 127.9 mA), with exception of the leaves sampled at Borgerhout (location 4) which only significantly differed from the leaf SIRM from the Kalmthoutse Heide (location 2). No significant difference of SIRM value was observed among the leaves sampled from the non-urban locations.

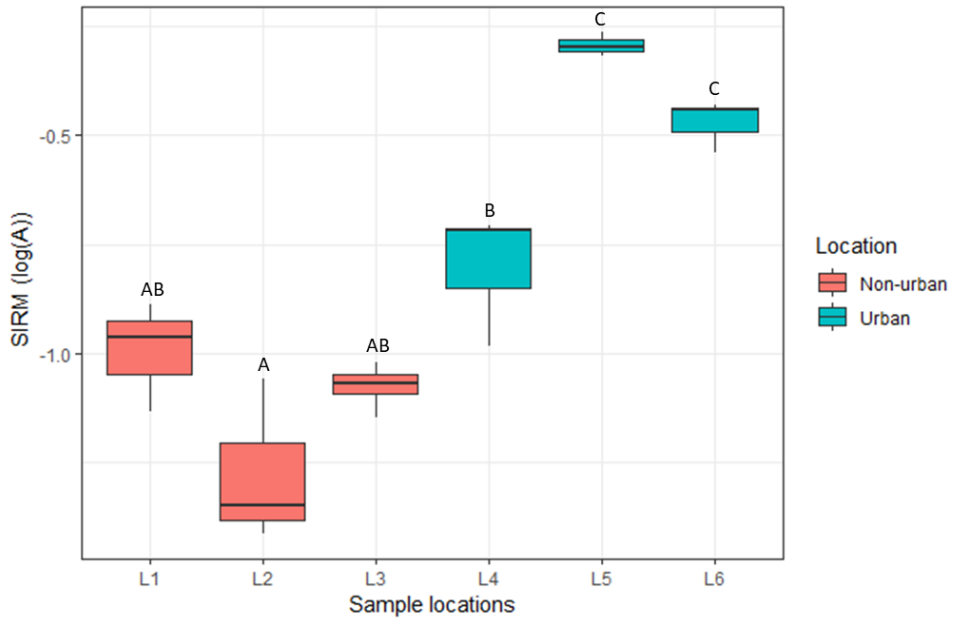

Figure 15. | **Leaf SIRM (mA) values of the ivy plant from 6 locations in the province of Antwerp**. Boxplots of SIRM Values containing the same letter (a, b, c) are not significantly different (α=0.05)

3.1.2 Determining the bacterial composition of phyllosphere communities

The composition of the microbial phyllosphere community found on the ivy samples was determined by 16S rRNA amplicon sequencing. A total of 157,871 sequence reads were obtained across all six leaf samples with an average of 2.66 ± 1.42 x 10^4 reads per sample. Based upon these generated gene sequences, corrected for leaf surface, and normalized by spike, an average of 4.13 ± 2.41 x 10^6 bacteria/cm² leaf was determined, which corresponds to literature (Laforest-Lapointe et al., 2017). After sequence assembly and filtering, a total of 1546 amplicon sequence variants (ASV) were generated (376.5 ± 109 ASVs per sample). Subsequently, the bacterial composition was analysed of the different samples. To compare general community differences, a principal coordinate analysis was performed (Fig. 16). The dimensional scaling of the Bray-Curtis dissimilarity matrix by two dimensions revealed that the communities clustered along the first principal coordinate axis (PCoA) into an urban and a non-urban cluster, explaining 49.6% of the variance. The second PCoA, explaining 22.2%, showed higher dissimilarity values between bacterial communities from urban samples in comparison to non-urban communities. The community composition of each sample was analysed at class, family, and

genus level (Fig. 17). *Alphaproteobacteria (Sphingomonas, Beijerinckiaceae, Acetobacteraceae, Novosphingobium, Methylobacterium), Cytophagia (Hymenobacter), betaproteobacteria (Massilia, Polaromonas), Sphingobacteriia (Mucilaginibacter), Deltaproteobacteria (DQ154856_g), Deinococci (Deinococcus), Cytophagia (Spirosoma), and Acidobacteriia (Edaphobacter)* were the overall most abundant bacterial species in urban and non-urban samples (Fig. 18) (>1% relative abundance of S16 rRNA sequence in all samples) with *Alphaproteobacteria* (49.0%), *Cytophagia* (16.0%), and Betaproteobacteria (7.66%) being the most abundant classes. As demonstrated in figure 15b, communities show a dramatic shift in many of the dominant taxa between urban and non-urban locations. The *Alphaproteobacteria* (*Beijerinckiaceae*) and *Acidobacteriia* (*Edaphobacter*) were primarily abundant in the non-urban samples, while the *Betaproteobacteria* (*Massilia* and *Noviherbaspirillum, Polaromonas*), *Sphingobacteriia* (*pedobacter*) and *Negativicutes* (*Veillonella*) were primarily abundant in the urban samples. Of the most common genera, *Massilia, Methylobacterium*, and *Sphingomonas* could be cultured and were therefore selected for further experiments.

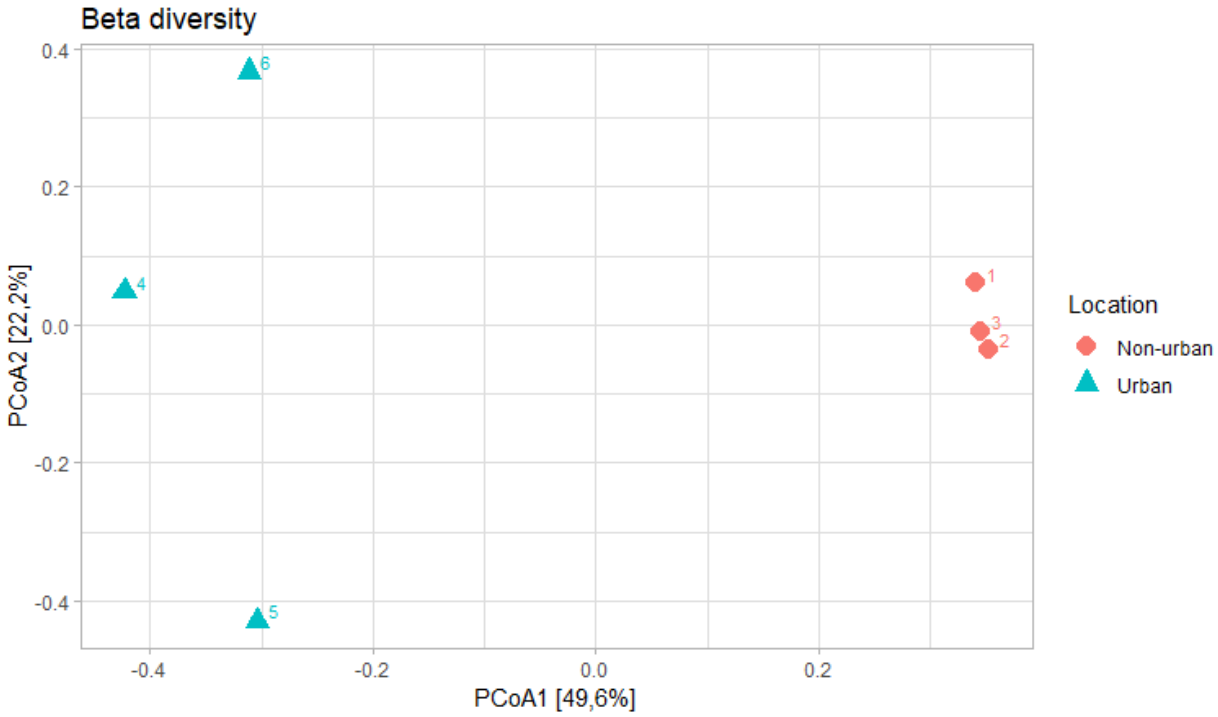

Figure 16. | Principal coordinate analysis ordination (PCoA) of the phyllosphere communities sampled at 6 different locations. Every point represents the bacterial community composition of one sample and the distance between these points refers to the dissimilarities between the communities. The urban and non-urban communities, espectively, are separated into two distinct groups. The number of labels indicates different samples within a sampling location highlighted in figure 11.

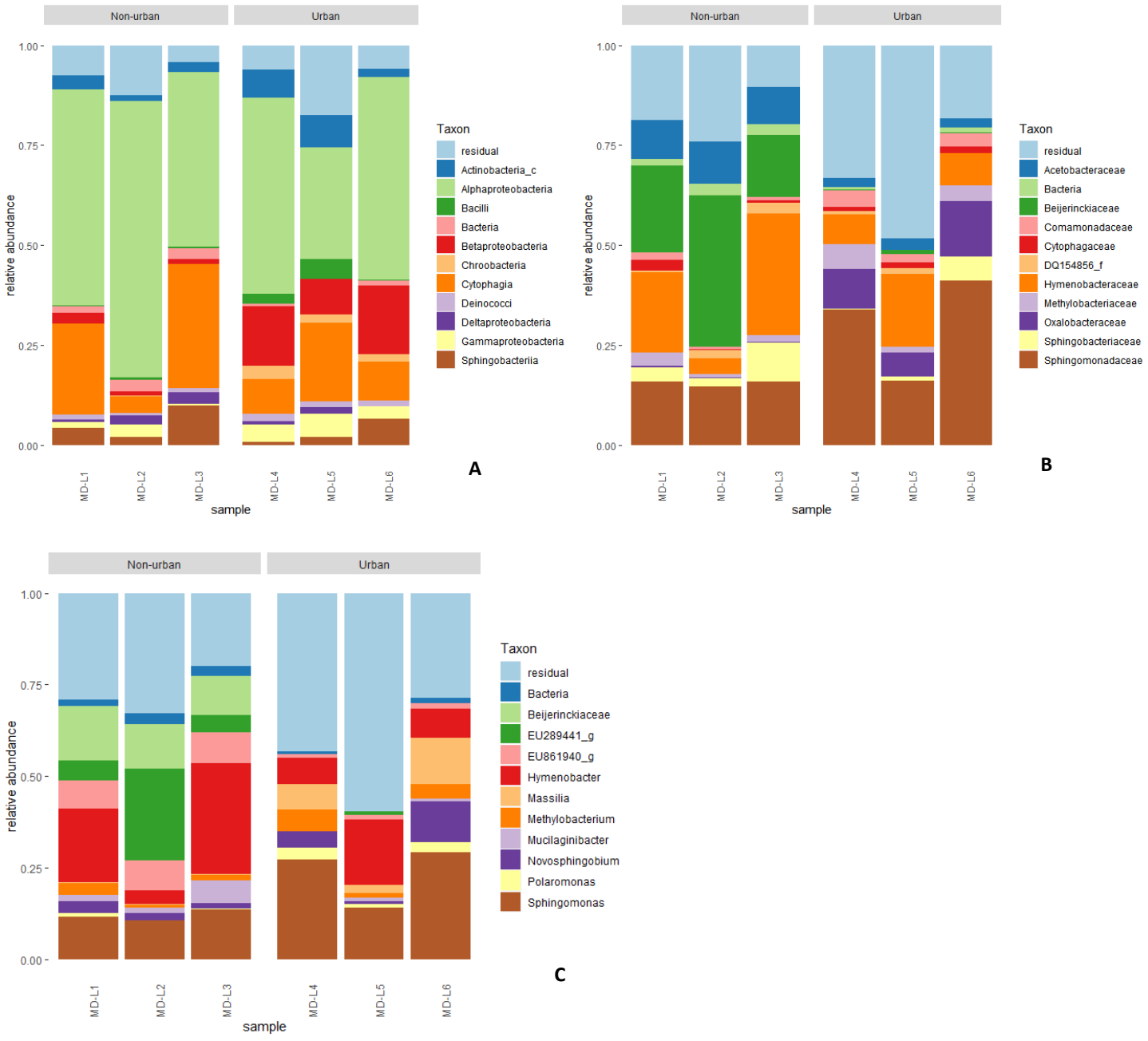

Figure 17. | Relative abundances of bacteria community proportions of six leaf samples. The different colours depict the different bacteria at the class (A), family (B), and genus level (C) level. The communities are separated by non-urban (MD-L1, MD-L2, MD-L3) and urban locations (MD-L4, MD-L5, MD-L6).

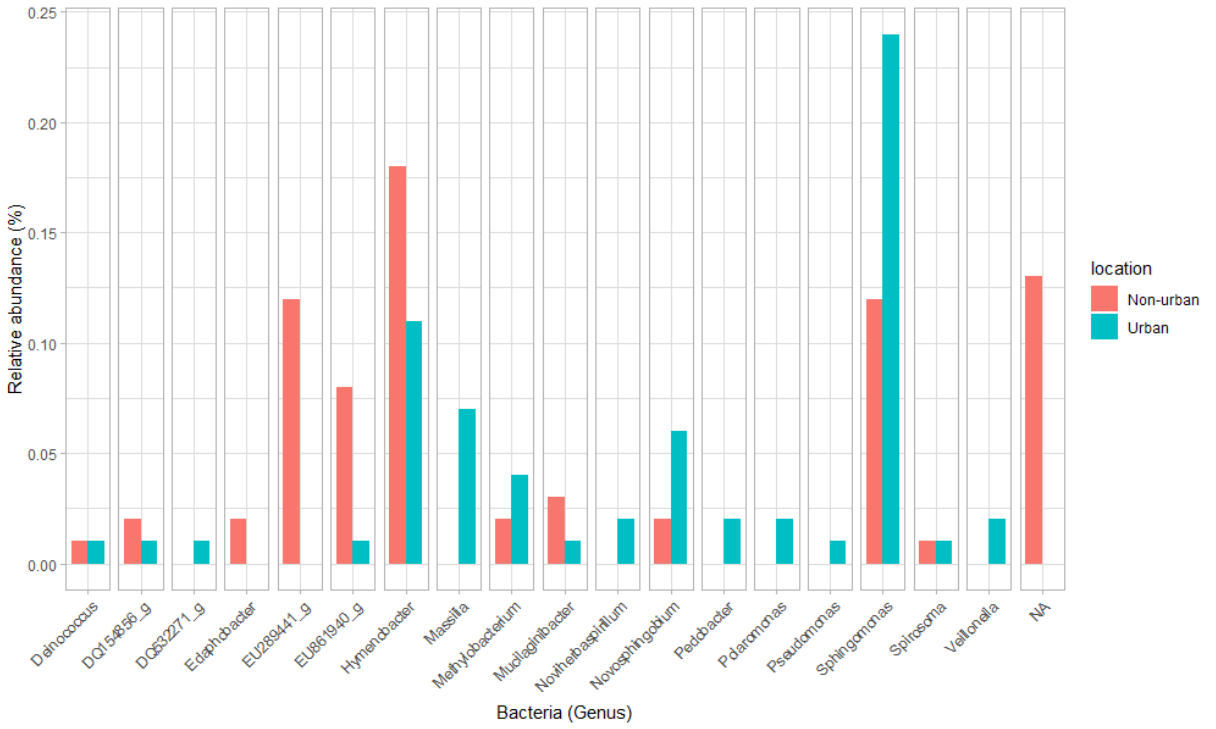

B

Figure 18. | Relative abundances of bacteria community proportions of six leaf samples at the genus level. The bar plot shows the relative abundance of the most abundant bacteria found in the communities of non-urban and urban locations.

3.1.3 *Leuconostoc* isolation from liquid manure

Among the isolates obtained from the liquid manure, *Leuconostoc mesenteroides* subsp. *jonggajibkimchii* was the only bacteria that could be identified by comparing the obtained 16s rRNA gene sequence to the EzBioCloud 16S rRNA gene database, downloaded on 08/01/2018 (Yoon et al., 2017). These bacteria have been characterized as non-spore-forming, facultatively anaerobic, Gram-positive bacteria with a cocci morphology without motilities (Jeon et al., 2017).

3.2 Biodegradation

In this section, the ability of the phyllosphere bacteria to individually bioremediate gaseous BTEX and NO_2 was explored and quantified.

3.2.1 Growth characterization

The growth phases of the phyllosphere bacteria in function of time were characterized via a bioscreen in order to standardize the measurements of the bioremediation capacity. In addition, the mean growth rate was determined relative to the positive control *Methylibium petroleiphilum* (Table 10 in appendix). Bacteria, such as Massilia suwonensis (2,068 ± 0.44), Methylobacterium gossipiicola/goesingense (1,84 ± 0,23), Nocardioides halotolerans (1,70 ± 0,29), and Massilia FAOS_s (1,87 ± 0,65) higher growth rate compared to the positive control Methylibium petroleiphilum. The growth rate was taken into account, among other things, when selecting additional bacteria for further experiments.

3.2.2 Tolbox optimization

To quantify the bioremediation capacity of phyllosphere bacteria, the bacteria were exposed to BTEX and NO_2 inside the Tolbox. Throughout the research period, the Tolbox and the protocol have been further modified and optimized. A new approach to flush the container has been installed which is

based upon pressurised air, resulting in decreased flushing time. As result, BTEX, taken up by the walls of the tolbox, had a limited time to release into the air before starting a new experiment, resulting in a shorter initial drop after the peak during measurements. A multichannel gas sensor has been installed which allows for the simultaneous measurement of carbon dioxide, NO_2, ethanol, hydrogen, ammonia, methane, propane, and iso-butane (Seeed Studio). Lastly, some additional steps have been implemented into the protocol (see 2.2.2. Bioremediation measurement). First, after the incubation period in the anaerobic jar, the plates were removed from the jar to let the BTEX in the plates desaturate before placing them in the Tolbox and second, the safety has been increased by closing of the glass vial containing BTEX during transport from the preparation site to the Tolbox.

3.2.3 Bioremediation capacity of 17 bacterial isolates

The selected bacteria for bioremediation are shown in Table 6. The capacity to degrade NO_2, benzene, toluene, ethylbenzene and the three isomers were tested for 17 bacterial isolates. The results shown below give an indication of bioremediation as the degradation was tested only once. Of these 17 bacterial isolates, bioremediation of BTEX was only detected in isolate F exposed to TEX (Fig.19A & B) and *Methylibium petroleiphilum* (Fig. 19E). However, when isolate F was exposed to BTEX no degradation was observed. *Methylibium petroleiphilum* degraded benzene, toluene, and o-xylene, but showed no bioremediation activity of ethylbenzene and m, p-xylene. The other bacteria showed a similar decrease as the blank. The results of the capacity of phyllosphere bacteria to bioremediate NO_x are not shown due to lack of data.

Bacterial species	**%Benzene removed**		**%Toluene removed**		**%ethylbenzene removed**		**% O-xylene removed**		**% M-, P-xylene removed**	
	12 h	24 h	12 h	24 h	12 h	24 h	12 h	24 h	12 h	24 h
Blank	8.5%		8.6%		9.5%		14.7%		13.2%	
Methylibium petroleiphilum*	38.6%	99.4%	23.2%	96.2%	12.7%	27.9%	15.5%	42.0%	13.0%	26.8%
Frigoribacterium faeni			13.9%	18.8%	14.4%	17.5%	15.5%	17.3%	14.4%	16.4%
Isolate F (TEX)			28.0%	46.6%	25.7%	39.8%	16.9%	33.9%	22.1%	36.3%
Isolate F (BTEX)	11.9%	20.1%	11.0%	18.6%	10.4%	14.0%	9.2%	13.1%	7.8%	12.4%
Leuconostoc mesenteroides			2.2%	14%	2.2%	13.2%	0.9%	17.1%	2.0%	13.1%
Microbacterium lemovicicum	6.6%	17%	6.1%	16.9%	6.8%	15.5%	7.4%	15.9%	8.8%	17.7%
Methylobacterium bullatum	10.6%	17.8%	11.0%	20.7%	10.6%	16.8%	8.8%	12.9%	8.5%	
Methylobacterium cerastii			12.0%	18.0%	11.3%	16.9%	8.3%	18.8%	11.0%	12.5%
Methylobacterium gossipiicola/goesingense			6.2%	11.0	2.6%	10.5%	6.5%	12.1%	3.4%	18.2%
Massilia suwonensis			5.3%		1.0%		1.7%		2.0%	12.8%
Massilia FAOS_s			7.4%		6.1%		6.7%		5.0%	
Nocardioides halotolerans			4.5%		2.7%		2.7%		2.5%	
Oerskovia paurometabola/jenensis			7.7%		3.5%		4.4%		4.4%	
Okibacterium fritillariae			7.6%		7.5%		4.4%		5.8%	
Rathayibacter festucae/caricis			4.6%	15.8%	3.5%	13.6%	4.0%	14.2%	5.2%	
Rhodococcus cerastii			9.5%		10.5%		14.0%		11.0%	14.6%
Rhodococcus cercidiphylli /fascians			4.6%		1.2%		1.8%		3.7%	
Sphingomonas melonis			17.7%		17.5%		22.8%		15.6%	

Table 6. | Percentage of BTEX removal efficiency by phyllosphere bacteria, 12 and 24 h after C_0. *%removal at 7h and 40h is shown instead of 12h and 24h respectively due to a technical error during measurements.

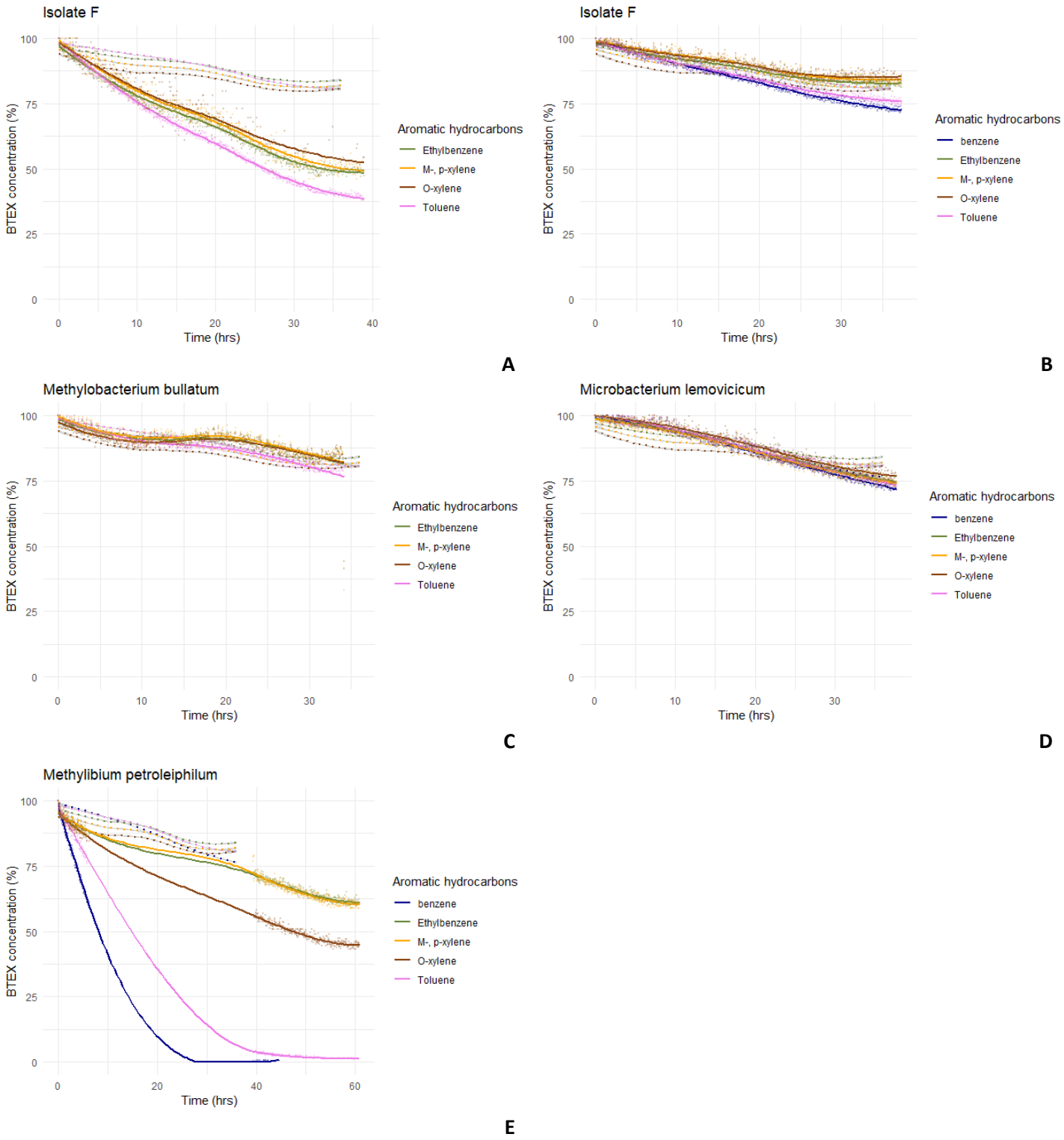

Figure 19. | Bioremediation of BTEX by plated bacteria: (A) Isolate F, (B) Isolate F, (C) *Methylobacterium bullatum,* (D) *Microbacterium lemovicicum*, (E) *Methylibium petroleiphilum*. The bacteria were exposed to benzene, toluene and ethylbenzene with an initial theoretical concentration of ±9.99 x 10^5 µg/m³ in the Tolbox. The concentration was measured over a period of 24 h to 48h. The graphs show the ambient concentration of BTEX exposed to phyllosphere bacteria as a solid line and a blank control as a dotted line.

3.3 Urban health

In order to determine the immuno-stimulating and/or -modulating potential of phyllosphere bacteria, selected from Table 1 and obtained via nettle manure isolation, phyllosphere bacteria were exposed to THP1-Dual™ cells and diesel particulate matter SRM1650B.

3.3.1 Influence of bacterial isolates on THP1-Dual cells

To determine the immune-inducing potential of phyllosphere bacteria, THP1-Dual cells were exposed to bacteria, which were selected on the ability to actively bioremediate air pollutants (Fig. 19), having a high relative growth rate or being the most abundant bacteria found in the phyllosphere communities (Fig. 18). From the available bacteria, eleven phyllosphere bacteria were selected, including *Massilia (suwonensis and neuiana), Methylibium petroleiphilum, Methylobacterium (gossipiicola/goesingense, bullatum, and pseudosasae/extorquens), Sphingomonas melonis, isolate F, Leuconostoc mesenteroides, Microbacterium lemovicicum*, and *Nocardioides halotolerans.* Fig. 17a (red boxplots) shows the median OD value of SEAP-reporter produced by THP1-Dual cells treated with bacteria. Nine out of 11 bacteria induced an increase in OD value indicating a direct effect of the bacterial strain on the production of NF-κB. A small but significant increase of immune response was observed when exposing THP1-Dual cells to *Nocardioides* ($p = 0.02$), *isolate F* ($p < 0.001$), *sphingomonas* ($p = 0.04$), *Microbacterium* ($p < 10^{-7}$), and *Methylobacterium bullatum* ($p < 10^{-7}$), while a significant increase ($p < 10^{-7}$) was measured after exposure of THP1-Dual cells to *Leuconostoc*, both *Massilia sp.* and *Methylibium petroleiphilum*. Of these bacteria, *Methylibium* (Gram-positive) and *Leuconostoc* (Gram-negative) induced respectively the highest and second-to-highest levels of immune response. *Methylobacterium gossipiicola/goesingense* and *pseudosasae/extorquens* showed no significant difference ($p = 0.99$) in OD value when compared to the negative control. *Methylobacterium bullatum* was the only bacterium which showed growth on the viability test and therefore wasn't killed by UV-radiation. A fraction of the 10^{-5} dilution, used in the THP1-Dual cell exposure (before UV-radiation), was plated to determine the true CFU concentration (Table 5).

3.3.2 Phyllosphere bacteria modulate the interaction between DEP and THP1-Dual cells

To determine whether phyllosphere bacteria can modulate DEP influence, THP1-Dual cells were treated with the selected bacteria and various concentrations of diesel particulate matter ranging from 0 to 100 µg/mL. When THP1-Dual cells were treated with no bacteria, stimulation with 50 and 100 µg/ml diesel showed a significant increase in SEAP production compared to 0 and 10 µg/mL diesel. A two-way ANOVA analysis showed a significant interaction effect between bacteria and diesel concentration on SEAP production ($p < 2 \times 10^{-16}$).

Three patterns were observed when phyllosphere bacteria and DEP were added to THP1-Dual cells (Fig. 20B). First, in THP1-Dual cells exposed to *isolate F, Methylobacterium gossipiicola/goesingense, Methylobacterium pseudosasae/extorquens*, *Microbacterium lemovicicum, Nocardioides halotolerans*, or *Sphingomonas melonis,* a co-stimulating (or even synergistic) effect on the SEAP production was observed in a concentration-dependent matter. Diesel concentrations of 50 and 100 µg/mL caused an overall significant increase in immune-response in combination with these bacteria. *Sphingomonas* or *Nocardioides* induced already a significant increase in SEAP production at a concentration of 10 µg/mL diesel. The second pattern occurred when THP1-Dual cells were exposed to *Massilia neuiena*, *Massilia suwonensis*, or *Methylobacterium bullatum*, which resulted in a non-significant difference in immune response between all the concentration of diesel particulate matter and the non-diesel-stimulated cells. A third pattern was observed for M*ethylibium petroleiphilum* and *Leuconostoc mesenteroides* which caused a statistically significant decrease in the immunological response with the increasing concentration of diesel particulate matter.

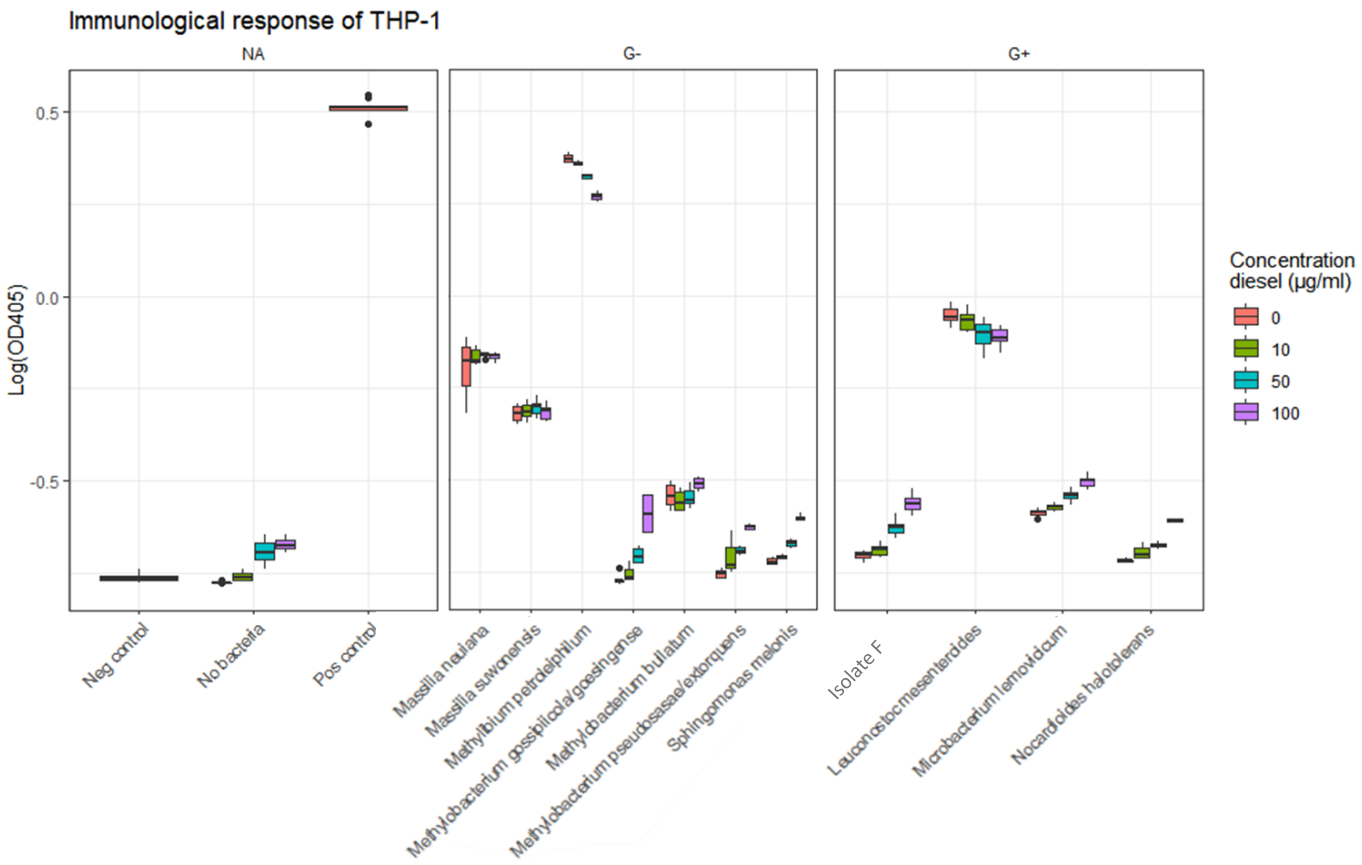
Immunological response of THP-1
NA
G-
G+
Log(OD405)
0.5
0.0
-0.5
Concentration diesel (µg/ml)
0
10
50
100
Neg control
No bacteria
Pos control
Massilia neuiana
Massilia suwonensis
Methylobium petroleiphilum
Methylobacterium gossipiicola/goesingense
Methylobacterium bullatum
Methylobacterium pseudosasae/extorquens
Sphingomonas melonis
Isolate F
Leuconostoc mesenteroides
Microbacterium lemovicum
Nocardioides halotolerans

A

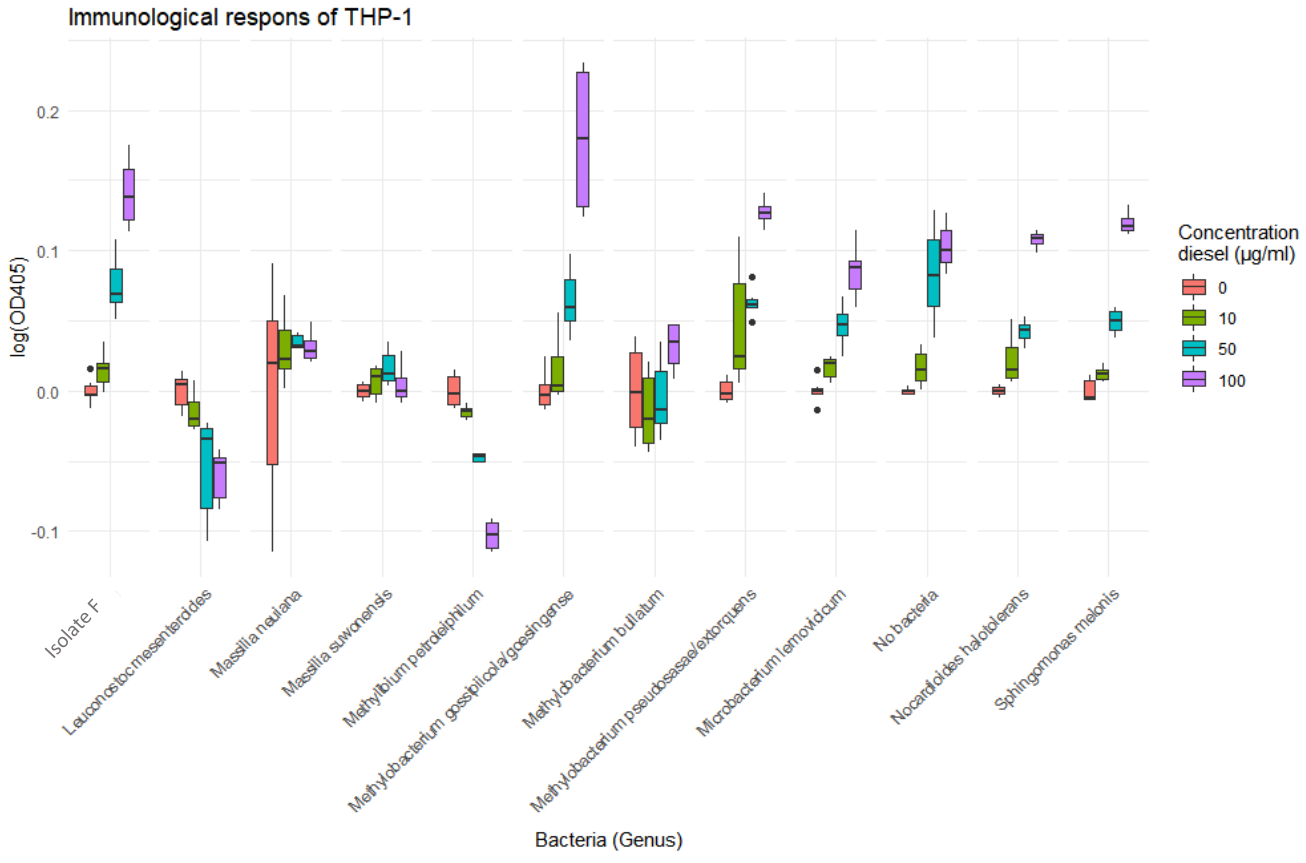
Immunological respons of THP-1
log(OD405)
0.2
0.1
0.0
-0.1
Concentration diesel (µg/ml)
0
10
50
100
Isolate F
Leuconostoc mesenteroides
Massilia neuiana
Massilia suwonensis
Methylobium petroleiphilum
Methylobacterium gossipiicola/goesingense
Methylobacterium bullatum
Methylobacterium pseudosasae/extorquens
Microbacterium lemovicum
No bacteria
Nocardioides halotolerans
Sphingomonas melonis
Bacteria (Genus)

B

Figure 20. (page above) | Immunological response of THP1-Dual cells to isolated bacteria and diesel particulate matter. The SEAP production as a result of the induction of the modified NF-kB-SEAP pathway over a period of 24 hrs is measured by adding pNPP. The measured OD values, as a result of the metabolised PNPP by SEAP, are expressed as log-transformed OD values. (A) The isolated bacteria are separated on the basis of gram stain and the different concentration of diesel particulate matter (0, 10, 50, 100 µg/mL) are visualised by colour. (B) The OD value of THP1-Dual cells exposed to no DEP was subtracted from the OD value generated by THP1-Dual cells exposed to the same bacteria to compare the interaction patterns of bacteria and DEP on THP1-Dual cells between bacteria. The different concentrations of diesel particulate matter (0, 10, 50, 100 µg/mL) are visualised by colour.

Bacteria	Experiment 1*	Experiment 2*
Massilia suwonensis	1.30E+02	4.09E+02
Leuconostoc mesenteroides		~1.67E+03
Methylibium petroleiphilum		~1.67E+03
Methylobacterium gossipiicola/goesingense		8.35E+01
Massilia neuiana	1.34E+04	~1.67E+03
Nocardioides halotolerans		3.84E+01
Isolate F	1.79E+02	2.97E+02
Methylobacterium bullatum	2.05E+03	~1.67E+03
Microbacterium lemovicicum	2.55E+02	6.45E+02
Methylobacterium pseudosasae/extorquens	3.67E+01	6.35E+01
Sphingomonas melonis	1.69E+02	6.15E+02

*(x 10^5 CFU/mL)

Table 5 | CFU/mL determined from the dilution used in the THP1-dual cell exposure experiment. Dilution 10^5 has been plated out to determine the end concentration CFU/mL added to the THP1-Dual cells. Concentration preceded with "~" are an estimate due to overgrowth and being unable to count the number of colonies.

Chapter 4: Discussion

4.1 Sampling

During this thesis, the mean leaf SIRM values were determined as an estimate for the difference in traffic-derived PM exposure between urban and non-urban areas and as indication for DEP exposure. The non-urban SIRM values were significantly lower than the urban SIRM values, with exception of the leaves sampled at Borgerhout (location 4) which only significantly differed from the SIRM from the Kalmthoutse Heide (location 2). These data suggest that air pollution in the urban areas we sampled is more magnetized compared to the non-urban areas we sampled. These results are in agreement with the overall higher concentration of air pollution found in urban areas (Mues et al., 2013, Smets et al., 2016, Vlaamse Milieumaatschapij, 2018). In Berchem, the presence of the train and the tram probably influenced the magnetic analysis as frictional processes of wheels, rails, and brakes strongly contribute to metals in particulate matter (Jiang et al., 2017).

The composition of phyllosphere communities on ivy leaves, sampled at 6 different location, were identified by means of 16S rRNA gene sequencing to give an indication of which are the most abundant bacteria. Both the urban and non-urban phyllosphere communities were dominated by the phylum *Alphaproteobacteria*, as was observed in previous studies (Laforest-Lapointe et al., 2017, Smets et al., 2016, Vorholt, 2012) followed by *Cytophagia*. *Sphingomonas* was the most dominant genus in urban locations and *Hymenobacter* in non-urban locations, while the *Hymenobacter* was previously identified as the most dominant taxa in urban locations and *Beijerinckia* in non-urban locations (Smets et al.,

2016). Our results of the ivy phyllosphere community show additional dominant phyllosphere bacteria (>1% relative abundance in all samples combined) to the phyllosphere community found by Smets et al. (2016) for ivy in this geographic region, such as *Betaproteobacteria* (*Massilia*), *Deinococci* (*Deinococcus*), *Cytophagia* (*Spirosoma*), *Proteobacteria* (*Edaphobacter*) and *Acidobacteriia* (*Edaphobacter*). Factors such as temperature, humidity and atmospheric pollutants have been suggested to play a role in the alteration of community composition (Smets et al., 2016).
Based on their high abundance in the phyllosphere, culturablility, and availability in the lab culture collection, the following bacterial isolates were selected for further experiments: *Massilia* sp., abundant in urban phyllosphere communities, and *Methylobacterium* sp., and *Sphingomonas* sp. abundant in urban and non-urban communities.

4.2 Biodegradation identification

In this study, we screened the bioremediation capacity of various strains isolated from the phyllosphere to degrade BTEX. After testing 17 different bacterial isolates, Isolate F gave an indication to effectively degrade toluene, ethylbenzene and xylene. Aside from the identification, no prior BTEX-degradative experiments were performed with these bacterial species to the best of our knowledge (Kim et al., 2014).
Isolate F, has been identified as an aerobic, Gram-positive, mesophilic, rodshaped and motile bacterium. To date, no experiments have been reported with the genus of isolate F in literature. Degradation was observed when isolate F was exposed to TEX but not to BTEX mixture. The decrease in the concentration of the TEX mixture, while the BTEX mixture remained constant, could be attributed to a leak in the setup at the time of the TEX exposure experiment. Another explanation could be the toxic and/or inhibitory effects of the BTEX mixture on the bacterium. Previous studies have shown that the degradation rate of each BTEX compound is highly influenced by other components (Yoshikawa et al., 2017). Reduction of BTEX degradation may occur because of the toxicity of by-products following the degradation of co-existing VOCs. To illustrate, catechol compounds are the main toxic by-products of BTEX degradation and are for example produced by *P. putida PPO1* during the degradation of p-xylene in the presence of benzene. Accumulation of these by-products from p-xylene degradation inhibits benzene degradation. 3-Methylcatechol, which is produced in the degradation pathway of toluene, o-xylene, and m-xylene, ceases the microbial growth when accumulated and limits toluene degradation by *P. putida strains* (Yoshikawa et al., 2017). Because additional repetitions of the experiment were not possible in the time frame of this thesis, the biodegradation capacity of isolate F must be confirmed in future studies.
Although we did not observe biodegradation capacity by *Microbacterium lemovicicium* (Fig. 16b) and *Rhodococcus* (*cerastii and cercidiphylli /fascians*), degradation has been found in members of the genus *Microbacterium* and *Rhodococcus.* In literature, *Microbacterium esteraromaticum,* and *Rhodococcus* (*rhodochrous* and strain *EC1*) have been found to bioremediate mixtures of BTEX as well as the separate compounds of the BTEX mixture (Wongbunmak et al., 2017a, Deeb and Alvarez-Cohen, 1999, Lee and Cho, 2008). Furthermore, degradation of BTEX by *Microbacterium* genera has been found in bacterial communities in BTEX-polluted groundwater (Cavalca et al., 2004) and in a toluene-enriched cultures (Su et al., 2014). However, it was not confirmed if the active degradation was due to the presence of *Microbacterium*. In contrast to these experiments, which were based on exposure of BTEX in liquid, we used a setup based on gaseous exposure. The absence of measured degradation may be due to other measurement conditions used in this study.

Although active degradation of BTEX was not observed by *Methylobacterium bullatum*, it is a promising bacterium due to other beneficial properties. Members of the genus *Methylobacterium*, identified as common leaf epiphytes, are known to use single carbon or multicarbon compounds with or without carbon-carbon bonds as a sole carbon source. (Dourado et al., 2015, Hoppe et al., 2011). These bacteria are able to promote plant growth by synthesizing growth-promoting phytohormones such as auxins and cytokinins, by degrading toxic organic compounds, immobilizing heavy metals and inhibiting plant pathogens (Dourado et al., 2015, Hoppe et al., 2011). In addition, the rod-shaped, Gram-negative, and strictly aerobic *M. bullatum* has the ability to form biofilms (Hoppe et al., 2011). Biofilm production allows bacteria to self-immobilize and develop tolerance to various physical, chemical and biological stressors such as high temperatures and drying (Kovaleva et al., 2014). If biodegradation is nevertheless confirmed in future studies, *M. bullatum* becomes an interesting bacteria for bioremediation in air cleaning techniques such as bioscrubbers and biotrickling filters (Delhomenie and Heitz, 2005). At the moment, bioremediation studies designed to test biofilm effectiveness in natural and artificial environments to clean VOCs are scarce (Lear and Lewis, 2012). However, some members of the genus *Methylobacterium* are known to be opportunistic bacteria to cause healthcare-associated colonization in medical devices and infection immunocompromised people (Kovaleva et al., 2014).

Methylibium petroleiphilum was identified to effectively degrade benzene and toluene and gave an indication of o-xylene degradation. Bioremediation of ethylbenzene, m-, and p-xylene was not observed. This could be explained by the absence of the necessary bioremediation pathways or by catabolite repression. Catabolite repression occurs when bacteria use a rapidly metabolizable carbon source first, in this case benzene and toluene, before other VOCs. To illustrate, succinate, which is a by-product of benzene and toluene degradation, is a rapidly metabolizable carbon source, which inhibits the degradation of xylene (Yoshikawa et al., 2017). The inability to bioremediate ethylbenzene is in contrast with previous studies. Nakatsu et al. (2006b) performed an experiment whereby *M. petroleiphilum* grown in mineral salt medium (MM) showed growth in the presence of ethylbenzene, benzene or toluene as sole carbon source. While *M. petroleiphilum,* exposed to xylene, resulted in the absence of growth, our study gave an indication of o-xylene degradation.

However, the degradation of all tested bacteria should be reconfirmed in future studies due to the lack of experimental repeats during this study. In addition, it should be noted that the concentration range used in this study (theoretical concentration of ±9.99 x 10^5 µg/m³) is much higher than naturally occurring concentrations (0-100 µg/m³; Hadei et al., 2018, Esplugues et al., 2010). Additional confirmation is needed in the future to evaluate the full potential and practicality of potentially interesting strains for bioremediation applications.

4.3 Urban Health

Phyllosphere bacteria are considered an important source of bioaerosols, which have important effects on human health (Jantunen et al., 2011, Bowers et al., 2010, Kim et al., 2018). Although a strong immune response by micro-organisms has the possibility of an inflammatory response that can cause tissue damage, which, however, is usually limited and does not have greater consequences for the host (Machado et al., 2004), micro-organisms can also provide immunoregulatory health benefits. Microorganisms, which induce immune responses, can immunomodulate the immune system and guide immunoregulation by for example inducing regulatory T-cells which attenuate allergic airway responses, and stimulating memory-phenotype T cells for viral antigens that the host has not been exposed to. Hereto, the immune system will be trained (Mills et al., 2017). Mills et al. (2017) hypothesized by introducing environmental micro-organisms into peoples urbanized environments, human health could benefit from the ecosystem service of immune protection and ultimately leading to decreased immune dysregulation. However the link between phyllosphere bacteria and health has not yet been investigated.

Therefore, the immune-inducing potential of phyllosphere bacteria was also determined aside from the bioremediation capacity to biodegrade BTEX mixtures. To assess the safety of usage of phyllosphere bacteria in bioremediation applications, the immune-inducing potential of phyllosphere bacteria were identified on THP1-Dual cells and the immune-modulating potential of these bacteria on the exposure of THP-1 dual cells to DEP. To our knowledge, no prior experiments investigating the interaction of phyllosphere bacteria and DEP on human cells have been performed. Hereto, bacteria were selected that showed active biodegradation, were abundant in the phyllosphere community, and/or showed a relative high growth rate. The isolate *Leuconostoc mesenteroides* from the nettle manure was also tested.

Methylibium petroleiphilum and *Leuconostoc mesenteroides* induced the highest production of NF-κB – and therefore the highest immune response - of all the tested bacteria. Remarkably, for some bacteria, when supplemented with increasing concentrations of DEP, the induction of NF-κB was reduced. The THP1-Dual cells exposed to *Massilia neuiena*, *Massilia suwonensis*, or *Methylobacterium bullatum* also resulted in an induction of NF-κB, but when supplemented with DEP resulted in neither an increase or a decrease of NF-κB production. Compared with the bacteria above, isolate F*, Methylobacterium gossipiicola/goesingense, Methylobacterium pseudosasae/extorquens*, *Microbacterium lemovicicum, Nocardioides halotolerans*, or *Sphingomonas melonis* induced a limited production of NF-κB in THP1-Dual cells. However when in the presence of DEP, a concentration-dependent increase of NF-κB production was observed. The exposure of THP1-Dual cells to only DEP showed an increase in induction. DEP are known to be pro-inflammatory explaining the increasing production of NF-κB production. Various bacteria have been found in literature to degrade PAHs, which could explain the stable NF-κB production with increasing DEP (Ghosal et al., 2016, Schwarze et al., 2013). However, the reduction in NF-kb production by THP1-Dual cells when combined with DEP and strong immune-inducing bacteria M*ethylibium petroleiphilum* or *Leuconostoc mesenteroides*, could not be explained based on the hypothesis. We initially hypothesized that phyllosphere bacteria could modulate the human immune response to the air pollutant DEP. Our results indicate that DEP can influence the interaction between phyllosphere bacteria and THP1-Dual cells. DEP have been shown in literature to upregulate pro-inflammatory mediators and antioxidant enzymes and to induce oxidative stress, altogether leading to inflammation in various cells (Schwarze et al., 2013, Baulig et al., 2003, Bonvallot et al., 2001, Lawal, 2018, Park et al., 2011, Jaguin et al., 2015). In addition, immunosuppressive effects by DEP on macrophages have also been reported (Dobrovolskaia and McNeil, 2016). Although the mechanism is poorly understood, the immunosuppression has been attributed to the depression of cytokine production and ROS expression after DEP exposure (Dobrovolskaia and McNeil, 2016, Jaguin et al., 2015). When applied to the observations, the pro-inflammatory influence of DEP can be observed in a concentration-dependent increase on the NF-kb production in the absence of bacteria or in the presence of weak immune-inducing bacteria. While in the presence of stronger immune-inducing bacteria, the immune suppressive ability of DEP becomes more prominent and can be observed by a decrease in NF-kb production. This would suggest that the pro-inflammatory effect of the bacteria and DEP and immunosuppressive effect of DEP cancel each other out as observed in the exposure of THP1-Dual cells to *Massilia neuiena*, *Massilia suwonensis*, or *Methylobacterium bullatum*. Exposure experiments, performed by Gurpreet (2013), showed that the observed effects were likely caused by the adsorbed compounds on SRM1650b (the type of DEP used) and not due to the elemental carbon of DEP. In addition, inflammation could not be attributed to endotoxin as none was adsorbed to SRM1650 (Gurpreet, 2013). In contrast to the findings mentioned above, a previous study which used the same standard reference material SRM1650b as DEP mixture found no stimulation of pro-inflamatory cytokines IL-6, CXCL8, TNF-α release after treatment of monocyte-derived macrophages (MDM) with SRM-1650B (Gurpreet, 2013), while other studies have shown that diesel particles cause the induction of several proinflammatory factors such as COX-2,

TNFα, C/EBPβ, IL-6, and IL-8 in human macrophages (Vogel et al., 2005). DEP extracts have been shown to increase pro-inflammatory cytokine expression in the human monocytic U937 cell line and to induce intracellular ROS generation through CYP system in human macrophages and human airway epithelial cells (Jaguin et al., 2015). It can be considered that the difference in cytokine profile from macrophages in DEP exposure studies is attributable to the surface chemistry of the particles. Immunosuppressive effects were highlighted in the study of Mundandhara et al. (2006). The study shows that 2-hr DEP-pre-treated alveolar macrophages significantly decreased in the ability to produce IL-1 and TNF-α in response to bacterial product LPS. Yang et al. (2003) showed short-term respiratory exposure of B6C3F1 mice to DEP resulted in systemic immunosuppression with evidence of T cell-mediated and possibly macrophage-mediated mechanisms. These observations of the pro-inflammatory and immunosuppressive abilities of DEP were further confirmed in other studies (Schwarze et al., 2013, Baulig et al., 2003, Bonvallot et al., 2001, Lawal, 2018, Park et al., 2011, Jaguin et al., 2015)
Moreover, further inflammation could be attributed to reactive oxygen species generated through UV-radiation of SRM1650 (to sterilize DEP) prior to the THP1-Dual cell exposure experiment. DEP followed the same protocol as the phyllosphere bacteria for UV-radiation prior to the exposure experiment. UV-radiation of PAHs adsorbed to the surface of DEP, which has been characterized by NIST (NIST, 2013), can initiate a series of excited state reactions leading to the formation of ROS and other reactive intermediates that can damage DNA, protein, and cell membrane, leading to acute toxicity and genotoxicity (Yu et al., 2006, Burchiel, 2005). DEP could furthermore have interfered with the phagocytosis of THP1-Dual cells. The particles were only sonicated for 2 minutes to disaggregate the particles. NIST reported a particle size distribution of 0.1 to 100 µm after 1hrs of sonification (fig 21 in appendix) (NIST, 2013).
A limitation of this study is the use of high exposure concentrations, compared to real-world situations. The exact levels to which pulmonary cells are likely to be exposed to *in vivo* are difficult to estimate, based on the complexity of DEP composition and the complexity of the deposition pattern in the lung. However, according to the estimations of Li et al. (2003), 1.4–143 µg/ml used in *in vitro* dose-response studies with macrophages is comparable to biologically tissue culture concentration ranging from 0.2 to 20 µg DEP/cm^2. This study uses concentrations in the same order of magnitude. However, compared to the average lung surface varying from 50 to 75 m^2 and the average ambient $PM_{2.5}$ concentration ranging from 12 to 17 µg/m^3 in Antwerp, it can be assumed that the DEP concentrations used in *in vitro* are higher than in *in vivo* situations.

4.4 Towards applications, and future research

In the current study, isolate F gave an indication to actively degrade BTEX, to induce a minimal immune reaction in THP-1 dual cells and to have a relatively low abundance (0.17%) in phyllosphere communities. In addition, no clinical cases were found caused by members of the genus of isolate F. If future experiments confirm the biodegradation capacity, isolate F could be enriched in phyllosphere communities to increase the naturally occurring low abundances.
Methylibium petroleiphilum, originally used as positive control for toluene degradation, indeed showed active degradation of toluene, benzene and o-xylene but showed no degradation of xylene and ethylbenzene. *M. petroleiphilum* was not found in phyllosphere communities. In literature, M. petroleiphilum was primarily found in soils contaminated with aromatic hydrocarbon (Nakatsu et al., 2006a). This would suggest that *M. petroleiphilum* is not adapted to the conditions found in the phyllosphere such as nutrient shortage, incident ultraviolet radiation and/or fluctuating moisture and pH levels (Lymperopoulou et al., 2016). Although the bacterium is not known to be pathogenic, *M. petroleiphilum* induced a strong immune reaction in THP-1 dual cells. As discussed above, an immune response has the possibility to induce inflammatory responses but can also provide immunoregulatory

health benefits (Machado et al., 2004, Mills et al., 2017). It would, therefore, be advised to do a safety analysis prior to the usage of the species in open bioremediation applications.
In contrast to *M. petroleiphilum* and isolate F, some bacteria, such as *Leuconostoc sp., Massilia sp., Methylobacterium sp., and Microbacterium* bacteria used during this thesis, have been reported in literature to be the cause in clinical cases, classifying them as opportunistic pathogens (Laffineur et al., 2003, Lai et al., 2011, Ballestero-Tellez et al., 2016, Ogier et al., 2008). Opportunistic pathogens could be a major problem in the clinical environment, limiting the applications of bioremediation in the presence of elderly and in health care related buildings due to immunocompromised patients (Ryan and Adley, 2010). Especially in the co-presence of DEP, as it could affect the pulmonary responses to phyllosphere bacteria due to the pro-inflammatory and immune-suppressing effects observed with THP1-Dual cells. A study by Harrod et al. (2004) found that prior exposure to inhaled DEP decreased lung bacterial clearance and exacerbated lung inflammation and injury to subsequent *Pseudomonas aeruginosa* infection. Furthermore, *Massilia sp.* might play a role in reduced urban air quality. *Massilia sp*. were primarily found in urban ivy leaf communities and were able to induce a relatively high immune response.
As discussed above, multiple experiments have already shown that exposure to a high diversity of bacteria early life reduces the incidence of developing an allergy in later life (Fujimura and Lynch, 2015). The lack of exposure could be addressed through the enrichment of the environment or via the use of probiotics. Based on the diversity hypothesis, it would be interesting to investigate if diversifying phyllosphere communities on plants, could reduce allergy development in early life. As phyllosphere bacteria influence a high fraction of the airborne microbial community, these bacteria could be acquired by the infant through natural routes including inhalation, skin contact, and swallowing (Lymperopoulou et al., 2016). This could be achieved by identifying the most common phyllosphere bacteria on house plants and thereafter introduce new beneficial phyllosphere bacteria to create a highly diverse indoor environment which enhances the microbial exposure. Community interventions, such as the activity of young mothers and children in urban agriculture or the increase of public green in urban areas, could inform this type of intervention strategy for the prevention of allergy development (Mills et al., 2017). The applications for probiotic prevention of allergic airway diseases have been previously studied but remain scarce (Spacova et al., 2018). Intervention studies testing for preventive effects of probiotics on allergic sensitization, eczema, wheezing illnesses, serum IgE levels, and asthma for a number of different probiotics species had controversial and varying results. For example, oral administration of probiotic strains such as the *Bifidobacterium longum* (Xiao et al., 2006), *Lactobacillus paracasei* (Wang et al., 2004), and *L. acidophilus* (Ishida et al., 2005) reduced the allergic symptoms after oral administration, while there was no benefit found by administrating *Lactobacillus rhamnosus* (Helin et al., 2002) or *Lactobacillus casei* (Tamura et al., 2007). On the other hand, intranasally administered *L. rhamnosus*, which showed no effect after oral administration, prevented the development of cardinal features of birch pollen-induced allergic asthma in a strain-specific manner (Spacova et al., 2019). *Leuconostoc mesenteroides* have been reported to be a promising probiotic against allergy in previous studies (Domingos Lopes et al., 2017). *Leuconostoc sp.* are generally recognized as safe because of their long history of usage in the dairy industry and their poor incidence in human infections cases, making *L. mesenteroides* a promising bacteria for further experiments as it was identified in the phyllosphere community (Ogier et al., 2008).

The following are some suggestions for future research and applications. As the phyllosphere bacteria were only measured once for BTEX degradation, repeated measurements are required to confirm the observed BTEX degradation ability of phyllosphere bacteria. In addition, to allow extrapolation of the lab tests to practical conditions, tests would have to take place in more realistic circumstances. Hereto, the bioremediation could be measured at a VOC concentration of 100 $\mu g/m^3$ that usually occurs

indoors (El-Hashemy and Ali, 2018a). An alternative screening method for active BTEX-degrading bacteria could be investigated which uses mineral salts medium (MM) enriched with ambient BTEX as sole carbon source. Using this setup, BTEX-degrading bacteria could be isolated from bacterial communities based on the forming of colonies. On the other hand, multiple bacterial strains plated separately on MM could be tested simultaneously for BTEX degradation in the Tolbox. By including the GC, a double evaluation could be performed by looking for bacterial growth on the plates and reduction in ambient concentration via the GC. Additional studies should be conducted to better understand the complex interactions of airborne bacteria and air pollution on human health.
Inoculation studies of the promising phyllosphere bacteria isolate F should be performed to investigate the best inoculation method for the highest survivability. Bacterial concentration should be followed up in time to see if the bacteria becomes stable in phyllosphere communities. Initial studies could be carried out with ivy leaves as the bacterial isolates were initially isolated from ivy. if successful, other house plants could be studied. Furthermore, it would be recommended to combine multiple bacteria for future applications because a single strain doesn't contain all the bioremediation pathways for complete remediation of BTEX mixtures.
If the benefit of phyllosphere bacteria is well substantiated and accepted by the general population, the usage of phyllosphere bacteria by health professionals, urban planners, architects, and restoration practitioners could be motivated to improve air quality and human health. House plants in occupational workplaces and houses, where the populations spends 90% of their time, could improve the general health. Different bacterial-plant combinations could be tested to investigate which combination best handles the parameters that are present in offices, living rooms, or classrooms for example.

In conclusion, air pollution is a serious global concern, therefore the development of effective bioremediation approaches, such as phylloremediation, is necessary. This study is, as far as we know, the first direct evidence of the TEX-degrading capacity of the non-pathogenic, mesophilic, phyllosphere bacterium Isolate F. In addition, phyllosphere bacteria induced different levels of NF-kb production in THP1-Dual cells of which Methylibium petroleiphilum and Leuconostoc mesenteroides induced the strongest reaction. Diesel exhaust particles were found to influence this interaction between phyllosphere bacteria and THP1 dual cells. The addition of DEP to strong immune-inducing bacteria reduced the NF-kB production in THP1-Dual cells, while addition of DEP to weak immune-inducing bacteria resulted in an increase of NF-kB production. The results of this study confirm the pro-inflammatory and immunosuppressive effect of DEP stated in literature. The outcome of this study may contribute to the development of new phylloremediation applications and to the understanding of the role of human-phyllosphere bacteria interaction in human health in relation to air pollution.

Appendix

Table 6 | The health effects of short-term and long-term BTEX exposure.

VOC	Short-term exposure	Long-term exposure
Benzene	asthma, dizziness, headaches, sensitization, fatigue, and lethargy (Wei et al., 2017)	aplastic anaemia, and decreased B-cell and T-cell proliferation (World Health Organization, 2010a)
Toluene		permanent incoordination, cognitive impairment, and vision or hearing loss (ATSDR, 2015)
Ethylbenzene	eye and throat irritation, vertigo, and dizziness (ATSDR, 2010)	long-term exposure studies in animals found irreversible damage to the inner ear and hearing, kidney damage, and an increase in kidney, liver and lung tumours (ATSDR, 2010)
Xylene	≥100 ppm: depression of the central nervous system, with symptoms such as headache, dizziness, nausea and vomiting ≥200 ppm: irritation of the lungs (causing chest pain and shortness of breath) Affect development of the foetus and can contaminate breast milk (Kandyala et al., 2010)	headaches, depression, insomnia, extreme tiredness, tremors, impaired concentration, and short-term memory loss (Kandyala et al., 2010)

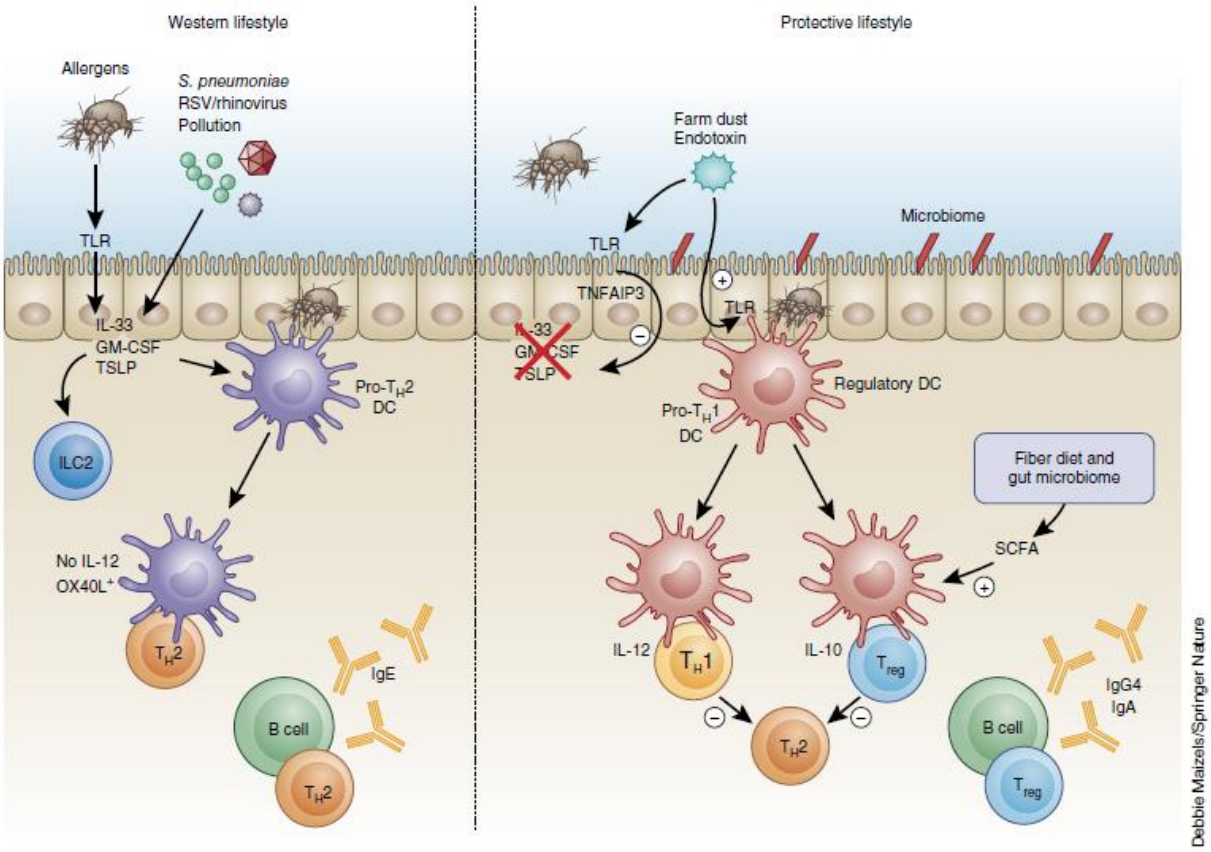

Figure 8 | Comparison of the immune-reaction pathway to allergen exposure in the epithelium in a western-lifestyle environment and a protective environment (Lambrecht and Hammad, 2017).

Genus	Species (closest relative if unknown)	Origin of Sample
Sphingomonas	melonis	Air
Rathayibacter	festucae/caricis	Ivy leaf
Okibacterium	fritillariae	Air
Rhodococcus	trifolii/LMRQ_s	Air
Methylobacterium	cerastii	
Methylobacterium	phyllostachyos	
Rhodococcus	cerastii	Ivy leaf
Williamsia	MJEJ_s	Ivy leaf
Erwinia	MTCH_s	Ivy leaf
Oerskovia	paurometabola/jenensis	Ivy leaf
Sphingomonas	desiccabilis	Ivy leaf
Massilia	neuiana	Ivy leaf
Gordonia		Ivy leaf
Methylobacterium	pseudosasae/extorquens	Ivy leaf
Paracoccus	chinensis	
Micromonospora	tulbaghiae	Ivy leaf
Streptomyces	bryophytorum	Ivy leaf
Methylobacterium	soli	Ivy leaf
Massilia	suwonensis	Ivy leaf
Isolate F		Ivy leaf
Massilia	FAOS_s	Ivy leaf
Microbacterium	lemovicicum	Ivy Leaf
Methylobacterium	adhaesivum	Ivy leaf
Methylobacterium	gnaphalii	Ivy leaf
Methylobacterium	gossipiicola/goesingense	Ivy leaf
Frigoribacterium	Faeni	Ivy leaf
Methylobacterium	bullatum	Ivy leaf
Nocardioides	halotolerans	Ivy leaf
Methylobacterium	pseudosasicola	Ivy leaf
Microbacterium	lacus	Ivy leaf
Micromonospora	saelicesensis	
Arthrobacter	gandavensis	Ivy leaf
Methylobacterium	extorquens	Ivy leaf
Streptomyces	*	Ivy leaf

Table 1. | Phyllosphere bacteria with their taxonomic classification and origin of sample. *Available sequence does not allow specific identification. Strain probably belongs to one of the following species: cyaneofuscatus/luridiscabiei/pratensis/cinereorecta/anulatus/fulvissimus/microflavus/fulvorobeus/griseus.

PAH	Mass Fraction(mg/kg)
Phenantherene	65.6 ± 3.6
1-Methylphenanthrene	32.1 ± 1.4
2-Methylphenanthrene	72.3 ± 1.2
3-Methylphenanthrene	56.7 ± 1.9
9-Methylphenanthrene	36.6 ± 1.6
Fluoranthene	48.1 ± 1.1
Pyrene	44.1 ± 1.2
Benzo[ghi]fluoranthene	11.1 ± 0.7
Benzo[c]phenanthrene	2.65 ± 0.24
Benz[a]anthracene	6.45 ± 0.39
Chrysene	13.4 ± 0.6
Triphenylene	9.49 ± 0.63
Benzo[a]fluoranthene	0.384 ± 0.023
Benzo[b]fluoranthene	6.77 ± 0.92
Benzo[j]fluoranthene	3.24 ± 0.50
Benzo[k]fluoranthene	2.30 ± 0.18
Benzo[e]pyrene	6.36 ± 0.37
Benzo[a]pyrene	1.25 ± 0.12
Perylene	0.167 ± 0.019
Indeno[1,2,3-cd]pyrene	4.48 ± 0.21
Benzo[ghi]perylene	6.04 ± 0.30
Dibenz[a,c]anthracene	0.493 ± 0.048
Dibenz[a,h]anthracene	0.365 ± 0.082
Dibenz[a,j]anthracene	0.387 ± 0.086
Benzo[b]chrysene	0.301 ± 0.019
Picene	0.506 ± 0.058

Table 8 | Certified Mass Fraction Values for PAHs in SRM 1650b. Concentrations of PAHs on the surface of SRM-1650B were analysed by using two or more analytical techniques. (NIST, 2013)

Nitro-PAH	Mass Fraction (µg/kg)
9-Nitrophenanthrene	539 ± 24
3-Nitrophenanthrene	4250 ± 50
2-Nitrofluoranthene	217 ± 15
3-Nitrofluoranthene	65.1 ± 1.1
1-Nitropyrene	18400 ± 300
7-Nitrobenz[a]anthracene	943 ± 22
6-Nitrochrysene	46.6 ± 1.1

Table 9 | Certified Mass Fraction Values for Nitro-PAHs in SRM 1650b. Concentrations of Nitro-PAHs on the surface of SRM-1650B were analysed by using two or more analytical techniques. (NIST, 2013)

Bacteria		Fitted value	Mean Doubling Time (hrs)	Mean Growth Rate		mean lag time (hrs)	
Erwinia	MTCH_s	3,17E-03	2,0	4,74	±2,35	0,3	
Frigoribacterium	faeni	4,48E-04	11,0	1,55	±1,20	30,7	±2,1
Isolate F		8,30E-04	10,4	1,31	±1,36	0,5	±0,2
Gordonia		2,25E-03	5,0	1,51	±0,15	3,7	
Leuconostoc	mesenteroides	2,72E-03	4,6	1,70	±0,19	2,0	
Massilia	FAOS_s	2,41E-03	5,9	1,87	±0,65	2,8	±0,2
Massilia	suwonensis	3,86E-03	4,3	2,07	±0,44	1,2	±0,7
Massilia	neuiana	6,04E-04	3,7	0,43	±0,04	0,7	
Methylibium	petroleiphilum	1,51E-03	4,5	1	±0,04	0,6	±0,2
Methylobacterium	adhaesivum	9,05E-04	4,3	0,68	±0,26	27,7	
Methylobacterium	gnaphalii	2,01E-03	3,8	1,21	±0,10	11,0	
Methylobacterium	gossipiicola/goesingense	2,46E-03	17,7	1,84	±0,23	5,0	
Methylobacterium	bullatum	1,24E-03	7,5	0,70	±0,28	10,3	±4,6
Methylobacterium	pseudosasicola	4,60E-04	12,2	0,34	±0,10	14,3	
Methylobacterium	pseudosasae/extorquens	1,18E-03	6,3	0,90	±0,13	8,3	±0,5
Methylobacterium	soli	1,35E-03	4,1	0,50	±0,33	25,1	±0,2
Methylobacterium	phyllostachyos	1,09E-03	12,5	0,79	±0,07	0	
Microbacterium	lacus	3,57E-03	23,3	2,38	±0,40	2,9	±0,2
Microbacterium	lemovicicum	1,83E-03	8,5	1,18	±0,17	0,2	±0,2
Nocardioides	halotolerans	2,81E-03	19,1	1,70	±0,29	0,2	±0,2
Oerskovia	paurometabola/jenensis	1,83E-03	9,6	1,27	±0,07	2,3	±0,3
Okibacterium	fritillariae	2,28E-03	3,2	1,51	±0,07	0,2	±0,2
Paracoccus	chinensis	1,39E-03	6,5	0,70	±0,22	4,8	±0,5
Rhodococcus	cerastii	8,03E-04	4,5	0,48	±0,04	0,4	±0,2
Rhodococcus	trifolii/LMRQ_s	8,74E-04	5,9	0,60	±0,05	0,6	±0,2
Sphingomonas	melonis	1,65E-03	5,0	1,37	±0,39	10,3	
Sphingomonas	desiccabilis	1,18E-03	11,5	0,71	±0,05	2,0	
Williamsia	MJEJ_s	1,17E-03	15,6	0,83	±0,09	0,1	±0,2
TolF49		2,88E-03	12,6	2,07	±0,19	2,0	
TolF51		1,12E-03	5,8	0,79	±0,07	15,0	
TolF53		2,66E-03	10,7	1,49	±0,84	3,8	±0,2

Table 10. | Bacterial growth characterization. Growth phases of the bacterial strains were determined via a bioscreen assay by measuring the turbidity of the growth medium over time. From the obtained data, the fitted value and mean doubling time of the exponential phase were calculated. The growth of the bacteria were compared to Methylibium petroleiphilum and expressed as the mean growth rate. No dat a is shown of bacteria where no growth was detected.

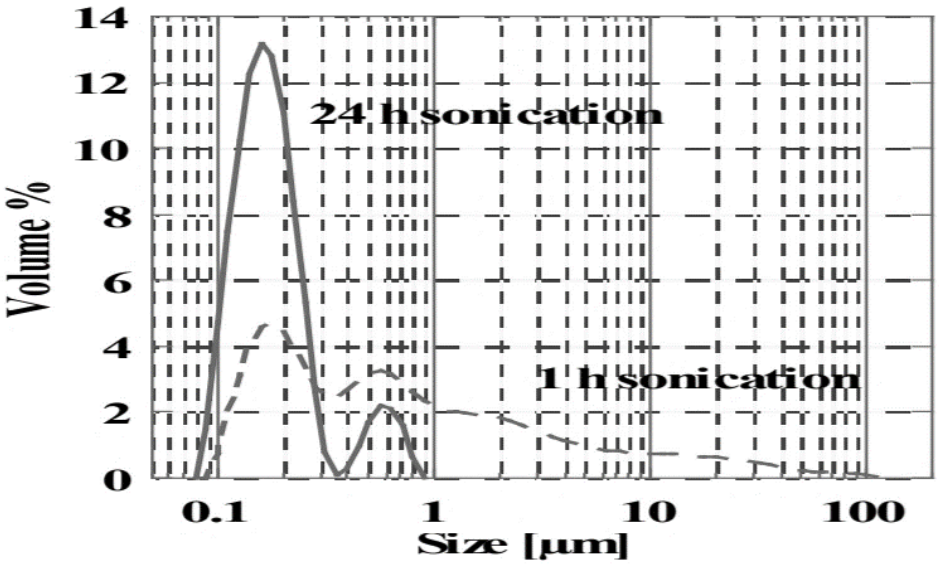

Figure 21 | Particle-size distribution for SRM 1650b after 1 h and 24 h sonication (NIST, 2013).

References

AKMIRZA, I., PASCUAL, C., CARVAJAL, A., PÉREZ, R., MUÑOZ, R. & LEBRERO, R. 2017. Anoxic biodegradation of BTEX in a biotrickling filter. *Science of The Total Environment,* 587-588**,** 457-465.

ANDREAE, D. & NOWAK-WĘGRZYN, A. 2017. Chapter 6 - The Effect of Infant Allergen/Immunogen Exposure on Long-Term Health. *In:* SAAVEDRA, J. M. & DATTILO, A. M. (eds.) *Early Nutrition and Long-Term Health.* Woodhead Publishing.

ATSDR 2010. PUBLIC HEALTH STATEMENT: Ethylbenzene.

ATSDR 2015. Public health statement. *In:* SCIENCES, D. O. T. A. H. H. (ed.).

AZUBUIKE, C. C., CHIKERE, C. B. & OKPOKWASILI, G. C. 2016. Bioremediation techniques-classification based on site of application: principles, advantages, limitations and prospects. *World journal of microbiology & biotechnology,* 32**,** 180-180.

BALLESTERO-TELLEZ, M., LABORDA GUIRAO, T., BATISTA DIAZ, N. & PASCUAL HERNANDEZ, A. 2016. First reported case of a corneal abscess caused by Massilia timonae. *Enferm Infecc Microbiol Clin,* 34**,** 212-3.

BATTAGLIA, M. A., JR., DOUGLAS, S. & HENNIGAN, C. J. 2017. Effect of the Urban Heat Island on Aerosol pH. *Environ Sci Technol,* 51**,** 13095-13103.

BAUER, R. N., DIAZ-SANCHEZ, D. & JASPERS, I. 2012. Effects of air pollutants on innate immunity: the role of Toll-like receptors and nucleotide-binding oligomerization domain-like receptors. *J Allergy Clin Immunol,* 129**,** 14-24; quiz 25-6.

BAULIG, A., SOURDEVAL, M., MEYER, M., MARANO, F. & BAEZA-SQUIBAN, A. 2003. Biological effects of atmospheric particles on human bronchial epithelial cells. Comparison with diesel exhaust particles. *Toxicol In Vitro,* 17**,** 567-73.

BONVALLOT, V., BAEZA-SQUIBAN, A., BAULIG, A., BRULANT, S., BOLAND, S., MUZEAU, F., BAROUKI, R. & MARANO, F. 2001. Organic compounds from diesel exhaust particles elicit a proinflammatory response in human airway epithelial cells and induce cytochrome p450 1A1 expression. *Am J Respir Cell Mol Biol,* 25**,** 515-21.

BOWERS, R. M., MCLETCHIE, S., KNIGHT, R. & FIERER, N. 2010. Spatial variability in airborne bacterial communities across land-use types and their relationship to the bacterial communities of potential source environments. *The Isme Journal,* 5**,** 601.

BURCHIEL, S. W. 2005. Polycyclic Aromatic Hydrocarbons (PAHs) and the Immune System. *In:* VOHR, H.-W. (ed.) *Encyclopedic Reference of Immunotoxicology.* Berlin, Heidelberg: Springer Berlin Heidelberg.

CAFARO, V., IZZO, V., SCOGNAMIGLIO, R., NOTOMISTA, E., CAPASSO, P., CASBARRA, A., PUCCI, P. & DI DONATO, A. 2004. Phenol hydroxylase and toluene/o-xylene monooxygenase from Pseudomonas stutzeri OX1: interplay between two enzymes. *Appl Environ Microbiol,* 70**,** 2211-9.

CALLAHAN, B. 2019. *DADA2 v.1.12* [Online]. Available: https://benjjneb.github.io/dada2/https://benjjneb.github.io/dada2/ [Accessed].

CAO, B., NAGARAJAN, K. & LOH, K.-C. 2009. *Biodegradation of aromatic compounds: Current status and opportunities for biomolecular approaches*.

CAVALCA, L., DELL'AMICO, E. & ANDREONI, V. 2004. Intrinsic bioremediability of an aromatic hydrocarbon-polluted groundwater: diversity of bacterial population and toluene monoxygenase genes. *Applied Microbiology and Biotechnology,* 64**,** 576-587.

CHANPUT, W., MES, J. J. & WICHERS, H. J. 2014. THP-1 cell line: An in vitro cell model for immune modulation approach. *International Immunopharmacology,* 23**,** 37-45.

CHEN, X., LIU, J., ZHOU, J., WANG, J., CHEN, C., SONG, Y. & PAN, J. 2018. Urban particulate matter (PM) suppresses airway antibacterial defence. *Respir Res,* 19**,** 5.

CHEN, Y. & WANG, F. 2015. Insights on nitrate respiration by Shewanella. *Frontiers in Marine Science,* 1.

CIBELLA, F., CUTTITTA, G., DELLA MAGGIORE, R., RUGGIERI, S., PANUNZI, S., DE GAETANO, A., BUCCHIERI, S., DRAGO, G., MELIS, M. R., LA GRUTTA, S. & VIEGI, G. 2015. Effect of indoor nitrogen dioxide on lung function in urban environment. *Environ Res,* 138**,** 8-16.

DE KEMPENEER, L., SERCU, B., VANBRABANT, W., VAN LANGENHOVE, H. & VERSTRAETE, W. 2004. Bioaugmentation of the phyllosphere for the removal of toluene from indoor air. *Appl Microbiol Biotechnol,* 64**,** 284-8.

DEEB, R. A. & ALVAREZ-COHEN, L. 1999. Temperature effects and substrate interactions during the aerobic biotransformation of BTEX mixtures by toluene-enriched consortia and Rhodococcus rhodochrous. *Biotechnol Bioeng,* 62**,** 526-36.

DELHOMENIE, M. C. & HEITZ, M. 2005. Biofiltration of air: a review. *Crit Rev Biotechnol,* 25**,** 53-72.

DELLI, A. J. & LERNMARK, Å. 2016. Chapter 39 - Type 1 (Insulin-Dependent) Diabetes Mellitus: Etiology, Pathogenesis, Prediction, and Prevention∗. *In:* JAMESON, J. L., DE GROOT, L. J., DE KRETSER, D. M., GIUDICE, L. C., GROSSMAN, A. B., MELMED, S., POTTS, J. T. & WEIR, G. C. (eds.) *Endocrinology: Adult and Pediatric (Seventh Edition).* Philadelphia: W.B. Saunders.

DOBROVOLSKAIA, M. & MCNEIL, S. E. 2016. *Handbook of immunological properties of engineered nanomaterials*.

DOMINGOS LOPES, M., NAGY, A., STANTON, C., ROSS, P. R., GELENCSÉR, E. & SILVA, C. 2017. *Immunomodulatory activity of exopolysaccharide producing Leuconostoc citreum strain isolated from Pico cheese*.

DOURADO, M. N., CAMARGO NEVES, A. A., SANTOS, D. S. & ARAUJO, W. L. 2015. Biotechnological and agronomic potential of endophytic pink-pigmented methylotrophic Methylobacterium spp. *Biomed Res Int,* 2015**,** 909016.

EISNER, A. D., RICHMOND-BRYANT, J., HAHN, I., DRAKE-RICHMAN, Z. E., BRIXEY, L. A., WIENER, R. W. & ELLENSON, W. D. 2009. Analysis of indoor air pollution trends and characterization of infiltration delay time using a cross-correlation method. *J Environ Monit,* 11**,** 2201-6.

EL-HASHEMY, M. A. & ALI, H. M. 2018a. Characterization of BTEX group of VOCs and inhalation risks in indoor microenvironments at small enterprises. *Sci Total Environ,* 645**,** 974-983.

EL-HASHEMY, M. A. & ALI, H. M. 2018b. Characterization of BTEX group of VOCs and inhalation risks in indoor microenvironments at small enterprises. *Science of The Total Environment,* 645**,** 974-983.

ESPLUGUES, A., BALLESTER, F., ESTARLICH, M., LLOP, S., FUENTES-LEONARTE, V., MANTILLA, E. & IÑIGUEZ, C. 2010. Indoor and outdoor air concentrations of BTEX and determinants in a cohort of one-year old children in Valencia, Spain. *Science of The Total Environment,* 409**,** 63-69.

FILLEUL, L., RONDEAU, V., VANDENTORREN, S., LE MOUAL, N., CANTAGREL, A., ANNESI-MAESANO, I., CHARPIN, D., DECLERCQ, C., NEUKIRCH, F., PARIS, C., VERVLOET, D., BROCHARD, P., TESSIER, J. F., KAUFFMANN, F. & BALDI, I. 2005. Twenty five year mortality and air pollution: results from the French PAARC survey. *Occup Environ Med,* 62**,** 453-60.

FRANKLIN, B. A., BROOK, R. & ARDEN POPE, C. 2015. Air Pollution and Cardiovascular Disease. *Current Problems in Cardiology,* 40**,** 207-238.

FROST & SULLIVAN 2016. Indoor Air Purification Technologies, Forecast to 2020.

FUJIMURA, K. E. & LYNCH, S. V. 2015. Microbiota in allergy and asthma and the emerging relationship with the gut microbiome. *Cell Host Microbe,* 17**,** 592-602.

FUJIYOSHI, S., TANAKA, D. & MARUYAMA, F. 2017. Transmission of Airborne Bacteria across Built Environments and Its Measurement Standards: A Review. *Front Microbiol,* 8**,** 2336.

FUKUDA, M., TAKEDA, H., KATO, H. E., DOKI, S., ITO, K., MATURANA, A. D., ISHITANI, R. & NUREKI, O. 2015. Structural basis for dynamic mechanism of nitrate/nitrite antiport by NarK. *Nat Commun,* 6**,** 7097.

GAUDERMAN, W. J., GILLILAND, G. F., VORA, H., AVOL, E., STRAM, D., MCCONNELL, R., THOMAS, D., LURMANN, F., MARGOLIS, H. G., RAPPAPORT, E. B., BERHANE, K. & PETERS, J. M. 2002. Association between air pollution and lung function growth in southern California children: results from a second cohort. *Am J Respir Crit Care Med,* 166**,** 76-84.

GEISS, O., GIANNOPOULOS, G., TIRENDI, S., BARRERO-MORENO, J., LARSEN, B. R. & KOTZIAS, D. 2011. The AIRMEX study-VOC measurements in public buildings and schools/kindergartens in eleven European cities: Statistical analysis of the data. *Atmospheric Environment,* 45**,** 3676-3684.

GHOSAL, D., GHOSH, S., DUTTA, T. K. & AHN, Y. 2016. Current State of Knowledge in Microbial Degradation of Polycyclic Aromatic Hydrocarbons (PAHs): A Review. *Front Microbiol,* 7**,** 1369.

GURPREET, S. 2013. *Diesel Exhaust Particles and Macrophage Function: Relevance to COPD.* PhD, Imperial College London.

HADEI, M., HOPKE, P. K., RAFIEE, M., RASTKARI, N., YARAHMADI, M., KERMANI, M. & SHAHSAVANI, A. 2018. Indoor and outdoor concentrations of BTEX and formaldehyde in Tehran, Iran: effects of building characteristics and health risk assessment. *Environmental Science and Pollution Research,* 25**,** 27423-27437.

HARROD, K. S., JARAMILLO, R. J., BERGER, J. A., GIGLIOTTI, A. P., SEILKOP, S. K. & REED, M. D. 2004. Inhaled Diesel Engine Emissions Reduce Bacterial Clearance and Exacerbate Lung Disease to Pseudomonas aeruginosa Infection In Vivo. *Toxicological Sciences,* 83**,** 155-165.

HASPESLAGH, E., HEYNDRICKX, I., HAMMAD, H. & LAMBRECHT, B. N. 2018. The hygiene hypothesis: immunological mechanisms of airway tolerance. *Current Opinion in Immunology,* 54**,** 102-108.

HELIN, T., HAAHTELA, S. & HAAHTELA, T. 2002. No effect of oral treatment with an intestinal bacterial strain, Lactobacillus rhamnosus (ATCC 53103), on birch-pollen allergy: a placebo-controlled double-blind study. *Allergy,* 57**,** 243-6.

HERIGSTAD, B., HAMILTON, M. & HEERSINK, J. 2001. How to optimize the drop plate method for enumerating bacteria. *Journal of Microbiological Methods,* 44**,** 121-129.

HOGE GEZONDHEIDSRAAD 2017. Indoor air quality in Belgium.

HOPPE, T., PETERS, K. & SCHMIDT, F. 2011. Methylobacterium bullatum sp. nov., a methylotrophic bacterium isolated from Funaria hygrometrica. *Systematic and Applied Microbiology,* 34**,** 482-486.

HRISTOVA, K. R., SCHMIDT, R., CHAKICHERLA, A. Y., LEGLER, T. C., WU, J., CHAIN, P. S., SCOW, K. M. & KANE, S. R. 2007. Comparative transcriptome analysis of Methylibium petroleiphilum PM1 exposed to the fuel oxygenates methyl tert-butyl ether and ethanol. *Appl Environ Microbiol,* 73**,** 7347-57.

HURST, C. J., CRAWFORD, R. L., GARLAND, J. L., LIPSON, D. A., MILLS, A. L. & STETZENBACH, L. D. 2007. *Manual of Environmental Microbiology, Third Edition*, American Society of Microbiology.

ISHIDA, Y., NAKAMURA, F., KANZATO, H., SAWADA, D., HIRATA, H., NISHIMURA, A., KAJIMOTO, O. & FUJIWARA, S. 2005. Clinical effects of Lactobacillus acidophilus strain L-92 on perennial allergic rhinitis: a double-blind, placebo-controlled study. *J Dairy Sci,* 88**,** 527-33.

JAGUIN, M., FARDEL, O. & LECUREUR, V. 2015. Exposure to diesel exhaust particle extracts (DEPe) impairs some polarization markers and functions of human macrophages through activation of AhR and Nrf2. *PLoS One,* 10**,** e0116560.

JANTUNEN, M., DE OLIVEIRA FERNANDES, E., CARRER, P. & KEPHALOPOULOS, S. 2011. *Promoting actions for healthy indoor air (IAIAQ)*.

JEON, H. H., KIM, K. H., CHUN, B. H., RYU, B. H., HAN, N. S. & JEON, C. O. 2017. A proposal of Leuconostoc mesenteroides subsp. jonggajibkimchii subsp. nov. and reclassification of Leuconostoc mesenteroides subsp. suionicum (Gu et al., 2012) as Leuconostoc suionicum sp. nov. based on complete genome sequences. *International Journal of Systematic and Evolutionary Microbiology,* 67**,** 2225-2230.

JI, B., YANG, K., ZHU, L., JIANG, Y., WANG, H., ZHOU, J. & ZHANG, H. 2015. Aerobic denitrification: A review of important advances of the last 30 years. *Biotechnology and Bioprocess Engineering,* 20**,** 643-651.

JIANG, S. Y., GALI, N. K., YANG, F., ZHANG, J. & NING, Z. 2017. Chemical characterization of size-segregated PM from different public transport modes and implications of source specific

contribution to public exposure. *Environmental Science and Pollution Research,* 24**,** 20029-20040.
JINDROVÁ, E., CHOCOVÁ, M., DEMNEROVÁ, K. & BRENNER, V. 2002. Bacterial aerobic degradation of benzene, toluene, ethylbenzene and xylene. *Folia Microbiologica,* 47**,** 83-93.
JONES, N. C., THORNTON, C. A., MARK, D. & HARRISON, R. M. 2000. Indoor/outdoor relationships of particulate matter in domestic homes with roadside, urban and rural locations. *Atmospheric Environment,* 34**,** 2603-2612.
KANDYALA, R., RAGHAVENDRA, S. P. C. & RAJASEKHARAN, S. T. 2010. Xylene: An overview of its health hazards and preventive measures. *Journal of oral and maxillofacial pathology : JOMFP,* 14**,** 1-5.
KARAKAS, B., LAKESTANI, S., GULER, C., GUCIZ DOGAN, B., ACAR VAIZOGLU, S., YOUSEFI RAD, A., SEKEREL, B., TıPıRDAMAZ, R. & GULLU, G. 2013. *Indoor and Outdoor Concentration of Particulate Matter at Domestic Homes*.
KARDEL, F., WUYTS, K., MAHER, B. A., HANSARD, R. & SAMSON, R. 2011. Leaf saturation isothermal remanent magnetization (SIRM) as a proxy for particulate matter monitoring: Inter-species differences and in-season variation. *Atmospheric Environment,* 45**,** 5164-5171.
KAWAI, T. & AKIRA, S. 2007. TLR signaling. *Seminars in Immunology,* 19**,** 24-32.
KAWASAKI, T. & KAWAI, T. 2014. Toll-like receptor signaling pathways. *Front Immunol,* 5**,** 461.
KEGG. 2019. *Nitrogen metabolism* [Online]. Kyoto Encyclopedia of Genes and Genomes. Available: https://www.genome.jp/kegg/ [Accessed 2019].
KEMBEL, S. W., O'CONNOR, T. K., ARNOLD, H. K., HUBBELL, S. P., WRIGHT, S. J. & GREEN, J. L. 2014. Relationships between phyllosphere bacterial communities and plant functional traits in a neotropical forest. *Proceedings of the National Academy of Sciences,* 111**,** 13715-13720.
KIM, K.-H., KABIR, E. & JAHAN, S. A. 2018. Airborne bioaerosols and their impact on human health. *Journal of Environmental Sciences,* 67**,** 23-35.
KIM, M., SINGH, D., LAI-HOE, A., GO, R., ABDUL RAHIM, R., AINUDDIN, A. N., CHUN, J. & ADAMS, J. M. 2012. Distinctive phyllosphere bacterial communities in tropical trees. *Microb Ecol,* 63**,** 674-81.
KIM, S. J., LIM, J. M., AHN, J. H., WEON, H. Y., HAMADA, M., SUZUKI, K., AHN, T. Y. & KWON, S. W. 2014. Description of Galbitalea soli gen. nov., sp. nov., and Frondihabitans sucicola sp. nov. *Int J Syst Evol Microbiol,* 64**,** 572-8.
KOVALEVA, J., DEGENER, J. E. & VAN DER MEI, H. C. 2014. Methylobacterium and its role in health care-associated infection. *J Clin Microbiol,* 52**,** 1317-21.
KOZICH, J. J., WESTCOTT, S. L., BAXTER, N. T., HIGHLANDER, S. K. & SCHLOSS, P. D. 2013. Development of a dual-index sequencing strategy and curation pipeline for analyzing amplicon sequence data on the MiSeq Illumina sequencing platform. *Appl Environ Microbiol,* 79**,** 5112-20.
LADINO-ORJUELA, G., GOMES, E., DA SILVA, R., SALT, C. & PARSONS, J. 2015. *Metabolic Pathways for Degradation of Aromatic Hydrocarbons by Bacteria*.
LAFFINEUR, K., AVESANI, V., CORNU, G., CHARLIER, J., JANSSENS, M., WAUTERS, G. & DELMEE, M. 2003. Bacteremia due to a novel Microbacterium species in a patient with leukemia and description of Microbacterium paraoxydans sp. nov. *J Clin Microbiol,* 41**,** 2242-6.
LAFOREST-LAPOINTE, I., MESSIER, C. & KEMBEL, S. W. 2016. Host species identity, site and time drive temperate tree phyllosphere bacterial community structure. *Microbiome,* 4**,** 27.
LAFOREST-LAPOINTE, I., MESSIER, C. & KEMBEL, S. W. 2017. Tree Leaf Bacterial Community Structure and Diversity Differ along a Gradient of Urban Intensity. *mSystems,* 2.
LAI, C. C., CHENG, A., LIU, W. L., TAN, C. K., HUANG, Y. T., CHUNG, K. P., LEE, M. R. & HSUEH, P. R. 2011. Infections caused by unusual Methylobacterium species. *J Clin Microbiol,* 49**,** 3329-31.
LAMBAIS, M. R., CROWLEY, D. E., CURY, J. C., BULL, R. C. & RODRIGUES, R. R. 2006. Bacterial diversity in tree canopies of the Atlantic forest. *Science,* 312**,** 1917.
LAMBRECHT, B. N. & HAMMAD, H. 2017. The immunology of the allergy epidemic and the hygiene hypothesis. *Nature Immunology,* 18**,** 1076.

LAWAL, A. O. 2018. Diesel Exhaust Particles and the Induction of Macrophage Activation and Dysfunction. *Inflammation,* 41**,** 356-363.
LEAR, G. & LEWIS, G. D. 2012. *Microbial Biofilms: Current Research and Applications*, Caister Academic Press.
LEE, E. H. & CHO, K. S. 2008. Characterization of cyclohexane and hexane degradation by Rhodococcus sp. EC1. *Chemosphere,* 71**,** 1738-44.
LEE, K. & GIBSON, D. T. 1996. Toluene and ethylbenzene oxidation by purified naphthalene dioxygenase from Pseudomonas sp. strain NCIB 9816-4. *Appl Environ Microbiol,* 62**,** 3101-6.
LI, N., HAO, M., PHALEN, R. F., HINDS, W. C. & NEL, A. E. 2003. Particulate air pollutants and asthma. A paradigm for the role of oxidative stress in PM-induced adverse health effects. *Clin Immunol,* 109**,** 250-65.
LINDOW, S. E. & BRANDL, M. T. 2003. Microbiology of the phyllosphere. *Appl Environ Microbiol,* 69**,** 1875-83.
LYMPEROPOULOU, D. S., ADAMS, R. I. & LINDOW, S. E. 2016. Contribution of Vegetation to the Microbial Composition of Nearby Outdoor Air. *Applied and environmental microbiology,* 82**,** 3822-3833.
LYNCH, S. V., WOOD, R. A., BOUSHEY, H., BACHARIER, L. B., BLOOMBERG, G. R., KATTAN, M., O'CONNOR, G. T., SANDEL, M. T., CALATRONI, A., MATSUI, E., JOHNSON, C. C., LYNN, H., VISNESS, C. M., JAFFEE, K. F., GERGEN, P. J., GOLD, D. R., WRIGHT, R. J., FUJIMURA, K., RAUCH, M., BUSSE, W. W. & GERN, J. E. 2014. Effects of early-life exposure to allergens and bacteria on recurrent wheeze and atopy in urban children. *J Allergy Clin Immunol,* 134**,** 593-601.e12.
MACHADO, P. R. L., ARAÚJO, M. I. A. S., CARVALHO, L. & CARVALHO, E. M. 2004. Mecanismos de resposta imune às infecções. *Anais Brasileiros de Dermatologia,* 79**,** 647-662.
MARTNER, A. 2018. *Regulation of innate and adaptive immune responses by Gram-positive and Gram-negative bacteria*.
MASIH, A., LALL, A. S., TANEJA, A. & SINGHVI, R. 2017. Exposure profiles, seasonal variation and health risk assessment of BTEX in indoor air of homes at different microenvironments of a terai province of northern India. *Chemosphere,* 176**,** 8-17.
METZGER, K. B., TOLBERT, P. E., KLEIN, M., PEEL, J. L., FLANDERS, W. D., TODD, K., MULHOLLAND, J. A., RYAN, P. B. & FRUMKIN, H. 2004. Ambient air pollution and cardiovascular emergency department visits. *Epidemiology,* 15**,** 46-56.
MEYSMAN, F. J. R. & DE CRAEMER, S. 2018. CurieuzeNeuzen Vlaanderen: Het cijferrapport. Universiteit Antwerpen.
MILLS, J. G., WEINSTEIN, P., GELLIE, N. J. C., WEYRICH, L. S., LOWE, A. J. & BREED, M. F. 2017. Urban habitat restoration provides a human health benefit through microbiome rewilding: the Microbiome Rewilding Hypothesis. *Restoration Ecology,* 25**,** 866-872.
MIRSKAYA, E. & E. AGRANOVSKI, I. 2018. *Sources and mechanisms of bioaerosol generation in occupational environments*.
MOIR, J. W. B. & WOOD, N. J. 2001. Nitrate and nitrite transport in bacteria. *Cellular and Molecular Life Sciences CMLS,* 58**,** 215-224.
MORETTI, S., SMETS, W., HOFMAN, J., MUBIANA, K. V., OERLEMANS, E., VANDENHEUVEL, D., SAMSON, R., BLUST, R. & LEBEER, S. 2019. Human inflammatory response of endotoxin affected by particulate matter-bound transition metals. *Environmental Pollution,* 244**,** 118-126.
MUES, A., MANDERS, A., SCHAAP, M., VAN ULFT, L. H., VAN MEIJGAARD, E. & BUILTJES, P. 2013. Differences in particulate matter concentrations between urban and rural regions under current and changing climate conditions. *Atmospheric Environment,* 80**,** 232-247.
MUNDANDHARA, S. D., BECKER, S. & MADDEN, M. C. 2006. Effects of diesel exhaust particles on human alveolar macrophage ability to secrete inflammatory mediators in response to lipopolysaccharide. *Toxicol In Vitro,* 20**,** 614-24.

MUÑOZ, R., MALHAUTIER, L., FANLO, J.-L. & QUIJANO, G. 2015. *Biological Technologies for the Treatment of Atmospheric Pollutants*.
NAKATSU, C. H., HRISTOVA, K., HANADA, S., MENG, X.-Y., HANSON, J. R., SCOW, K. M. & KAMAGATA, Y. 2006a. Methylibium petroleiphilum gen. nov., sp. nov., a novel methyl tert-butyl ether-degrading methylotroph of the Betaproteobacteria. *International Journal of Systematic and Evolutionary Microbiology,* 56**,** 983-989.
NAKATSU, C. H., HRISTOVA, K., HANADA, S., MENG, X. Y., HANSON, J. R., SCOW, K. M. & KAMAGATA, Y. 2006b. Methylibium petroleiphilum gen. nov., sp. nov., a novel methyl tert-butyl ether-degrading methylotroph of the Betaproteobacteria. *Int J Syst Evol Microbiol,* 56**,** 983-9.
NAZAROFF, W. W. 2016. Indoor bioaerosol dynamics. *Indoor Air,* 26**,** 61-78.
NIST 2013. Certificate of Analysis. *Standard Reference Material 1650b.* National Institute of Standards & Technology.
OGIER, J. C., CASALTA, E., FARROKH, C. & SAIHI, A. 2008. Safety assessment of dairy microorganisms: the Leuconostoc genus. *Int J Food Microbiol,* 126**,** 286-90.
OLIVARES, J., BEDMAR, E. J. & SANJUAN, J. 2013. Biological nitrogen fixation in the context of global change. *Mol Plant Microbe Interact,* 26**,** 486-94.
OLTRA, C., SALA, R., BOSO, À. & ASENSIO, S. L. 2017. Public engagement on urban air pollution: an exploratory study of two interventions. *Environmental Monitoring and Assessment,* 189**,** 296.
OWNBY, D. R., JOHNSON, C. C. & PETERSON, E. L. 2002. Exposure to dogs and cats in the first year of life and risk of allergic sensitization at 6 to 7 years of age. *Jama,* 288**,** 963-72.
PADHI, S. K. & GOKHALE, S. 2017. Treatment of gaseous volatile organic compounds using a rotating biological filter. *Bioresource Technology,* 244**,** 270-280.
PARK, E.-J., ROH, J., KANG, M.-S., KIM, S. N., KIM, Y. & CHOI, S. 2011. Biological Responses to Diesel Exhaust Particles (DEPs) Depend on the Physicochemical Properties of the DEPs. *PLOS ONE,* 6**,** e26749.
PAULIN, L. & HANSEL, N. 2016. Particulate air pollution and impaired lung function. *F1000Res,* 5.
QIN, Z. 2012. The use of THP-1 cells as a model for mimicking the function and regulation of monocytes and macrophages in the vasculature. *Atherosclerosis,* 221**,** 2-11.
R CORE TEAM. 2018. A Language and Environment for Statistical Computing. Available: https://www.r-project.org/.
RAHMAN, M. M. & MCFADDEN, G. 2011. Modulation of NF-κB signalling by microbial pathogens. *Nat Rev Microbiol,* 9**,** 291-306.
REDFORD, A. J., BOWERS, R. M., KNIGHT, R., LINHART, Y. & FIERER, N. 2010. The ecology of the phyllosphere: geographic and phylogenetic variability in the distribution of bacteria on tree leaves. *Environ Microbiol,* 12**,** 2885-93.
REDFORD, A. J. & FIERER, N. 2009. Bacterial succession on the leaf surface: a novel system for studying successional dynamics. *Microb Ecol,* 58**,** 189-98.
RYAN, M. P. & ADLEY, C. C. 2010. Sphingomonas paucimobilis: a persistent Gram-negative nosocomial infectious organism. *Journal of Hospital Infection,* 75**,** 153-157.
SALTHAMMER, T., SCHIEWECK, A., GU, J., AMERI, S. & UHDE, E. 2018. Future trends in ambient air pollution and climate in Germany – Implications for the indoor environment. *Building and Environment,* 143**,** 661-670.
SCHRODER, P. C., LI, J., WONG, G. W. & SCHAUB, B. 2015. The rural-urban enigma of allergy: what can we learn from studies around the world? *Pediatr Allergy Immunol,* 26**,** 95-102.
SCHWARZE, P. E., TOTLANDSDAL, A. I., LÅG, M., REFSNES, M., HOLME, J. A. & ØVREVIK, J. 2013. Inflammation-related effects of diesel engine exhaust particles: studies on lung cells in vitro. *Biomed Res Int,* 2013**,** 685142.
SHRIVASTAVA, R. & PHALE, P. 2012. Biodegradation of Mono-aromatic Compounds by Bacteria.
SIEGEL, J. A. 2016. Primary and secondary consequences of indoor air cleaners. *Indoor Air,* 26**,** 88-96.
SINGH, P., JAIN, R., SRIVASTAVA, N., BORTHAKUR, A., PAL, D. B., SINGH, R., SRIVASTAVA, P., TIWARY, D. & MISHRA, P. 2017. *Current and emerging trends in bioremediation of petrochemical waste: A review*.

SMETS, W., WUYTS, K., OERLEMANS, E., WUYTS, S., DENYS, S., SAMSON, R. & LEBEER, S. 2016. Impact of urban land use on the bacterial phyllosphere of ivy (Hedera sp.). *Atmospheric Environment,* 147**,** 376-383.

SPACOVA, I., CEUPPENS, J. L., SEYS, S. F., PETROVA, M. I. & LEBEER, S. 2018. Probiotics against airway allergy: host factors to consider. *Dis Model Mech,* 11.

SPACOVA, I., PETROVA, M. I., FREMAU, A., POLLARIS, L., VANOIRBEEK, J., CEUPPENS, J. L., SEYS, S. & LEBEER, S. 2019. Intranasal administration of probiotic Lactobacillus rhamnosus GG prevents birch pollen-induced allergic asthma in a murine model. *Allergy,* 74**,** 100-110.

SRIPRAPAT, W., SUKSABYE, P., AREEPHAK, S., KLANTUP, P., WARAHA, A., SAWATTAN, A. & THIRAVETYAN, P. 2014. Uptake of toluene and ethylbenzene by plants: Removal of volatile indoor air contaminants. *Ecotoxicology and Environmental Safety,* 102**,** 147-151.

STEIN, L. Y. & KLOTZ, M. G. 2016. The nitrogen cycle. *Curr Biol,* 26**,** R94-8.

SU, Y., XIA, F.-F., TIAN, B.-H., LI, W. & HE, R. 2014. Microbial community and function of enrichment cultures with methane and toluene. *Applied Microbiology and Biotechnology,* 98**,** 3121-3131.

TAKEUCHI, O. & AKIRA, S. 2010. Pattern recognition receptors and inflammation. *Cell,* 140**,** 805-20.

TAMURA, M., SHIKINA, T., MORIHANA, T., HAYAMA, M., KAJIMOTO, O., SAKAMOTO, A., KAJIMOTO, Y., WATANABE, O., NONAKA, C., SHIDA, K. & NANNO, M. 2007. Effects of probiotics on allergic rhinitis induced by Japanese cedar pollen: randomized double-blind, placebo-controlled clinical trial. *Int Arch Allergy Immunol,* 143**,** 75-82.

TAO, Y., FISHMAN, A., BENTLEY, W. E. & WOOD, T. K. 2004. Oxidation of benzene to phenol, catechol, and 1,2,3-trihydroxybenzene by toluene 4-monooxygenase of Pseudomonas mendocina KR1 and toluene 3-monooxygenase of Ralstonia pickettii PKO1. *Appl Environ Microbiol,* 70**,** 3814-20.

THOMPSON, A., RUDOLPH, J., ROHRER, F. & STEIN, O. 2003. *Concentration and stable carbon isotopic composition of ethane and benzene using a global three-dimensional isotope inclusive chemical tracer model*.

THULIN, M. 2018. *BAT: an online tool for analysing growth curves* [Online]. Available: http://www.mansthulin.se/bat/ [Accessed].

TIETZE, K., DALPKE, A., MORATH, S., MUTTERS, R., HEEG, K. & NONNENMACHER, C. 2006. Differences in innate immune responses upon stimulation with gram-positive and gram-negative bacteria. *J Periodontal Res,* 41**,** 447-54.

VAN DEN BERG, E. M., VAN DONGEN, U., ABBAS, B. & VAN LOOSDRECHT, M. C. 2015. Enrichment of DNRA bacteria in a continuous culture. *Isme j,* 9**,** 2153-61.

VENTURI, V. & KEEL, C. 2016. Signaling in the Rhizosphere. *Trends in Plant Science,* 21**,** 187-198.

VLAAMSE MILIEUMAATSCHAPIJ 2018. Jaarrapport Lucht. Emissies 2000-2016 en luchtkwaliteit 2017.

VOGEL, C. F., SCIULLO, E., WONG, P., KUZMICKY, P., KADO, N. & MATSUMURA, F. 2005. Induction of proinflammatory cytokines and C-reactive protein in human macrophage cell line U937 exposed to air pollution particulates. *Environ Health Perspect,* 113**,** 1536-41.

VOKOU, D., VARELI, K., ZARALI, E., KARAMANOLI, K., CONSTANTINIDOU, H.-I. A., MONOKROUSOS, N., HALLEY, J. M. & SAINIS, I. 2012. Exploring Biodiversity in the Bacterial Community of the Mediterranean Phyllosphere and its Relationship with Airborne Bacteria. *Microbial Ecology,* 64**,** 714-724.

VON HERTZEN, L., HANSKI, I. & HAAHTELA, T. 2011. Natural immunity. Biodiversity loss and inflammatory diseases are two global megatrends that might be related. *EMBO Rep,* 12**,** 1089-93.

VORHOLT, J. A. 2012. Microbial life in the phyllosphere. *Nature Reviews Microbiology,* 10**,** 828.

WANG, M. F., LIN, H. C., WANG, Y. Y. & HSU, C. H. 2004. Treatment of perennial allergic rhinitis with lactic acid bacteria. *Pediatr Allergy Immunol,* 15**,** 152-8.

WEI, X., LYU, S., YU, Y., WANG, Z., LIU, H., PAN, D. & CHEN, J. 2017. Phylloremediation of Air Pollutants: Exploiting the Potential of Plant Leaves and Leaf-Associated Microbes. *Frontiers in plant science,* 8**,** 1318-1318.

WEST, A. P., KOBLANSKY, A. A. & GHOSH, S. 2006. Recognition and signaling by toll-like receptors. *Annu Rev Cell Dev Biol,* 22**,** 409-37.

WILSON, M. & LINDOW, S. E. 1994. Coexistence among Epiphytic Bacterial Populations Mediated through Nutritional Resource Partitioning. *Applied and environmental microbiology,* 60**,** 4468-4477.

WITTOUCK, S. 2019. *Tidyamplicons* [Online]. Available: https://github.com/SWittouck/tidyamplicons/ [Accessed 14 March 2019].

WONGBUNMAK, A., KHIAWJAN, S., SUPHANTHARIKA, M. & PONGTHARANGKUL, T. 2017a. BTEX- and naphthalene-degrading bacterium Microbacterium esteraromaticum strain SBS1-7 isolated from estuarine sediment. *Journal of Hazardous Materials,* 339**,** 82-90.

WONGBUNMAK, A., KHIAWJAN, S., SUPHANTHARIKA, M. & PONGTHARANGKUL, T. 2017b. BTEX- and naphthalene-degrading bacterium Microbacterium esteraromaticum strain SBS1-7 isolated from estuarine sediment. *J Hazard Mater,* 339**,** 82-90.

WORLD HEALTH ORGANIZATION 2010a. Exposure to benzene: A major public health concern.

WORLD HEALTH ORGANIZATION 2010b. *WHO guidelines for indoor air quality: selected pollutants*.

XIAO, J. Z., KONDO, S., YANAGISAWA, N., TAKAHASHI, N., ODAMAKI, T., IWABUCHI, N., MIYAJI, K., IWATSUKI, K., TOGASHI, H., ENOMOTO, K. & ENOMOTO, T. 2006. Probiotics in the treatment of Japanese cedar pollinosis: a double-blind placebo-controlled trial. *Clin Exp Allergy,* 36**,** 1425-35.

YANG, H. M., BUTTERWORTH, L., MUNSON, A. E. & JEAN MEADE, B. 2003. *Respiratory exposure to diesel exhaust particles decreases the spleen IgM response to T cell-dependent antigen in female B6C3F1 mice*.

YANG, L., HOU, X.-Y., WEI, Y., THAI, P. & CHAI, F. 2017. Biomarkers of the health outcomes associated with ambient particulate matter exposure. *Science of The Total Environment,* 579**,** 1446-1459.

YOON, S. H., HA, S. M., KWON, S., LIM, J., KIM, Y., SEO, H. & CHUN, J. 2017. Introducing EzBioCloud: a taxonomically united database of 16S rRNA gene sequences and whole-genome assemblies. *Int J Syst Evol Microbiol,* 67**,** 1613-1617.

YOSHIKAWA, M., ZHANG, M. & TOYOTA, K. 2017. Biodegradation of Volatile Organic Compounds and Their Effects on Biodegradability under Co-Existing Conditions. *Microbes Environ,* 32**,** 188-200.

YU, H., XIA, Q., YAN, J., HERRENO-SAENZ, D., WU, Y. S., TANG, I. W. & FU, P. P. 2006. Photoirradiation of polycyclic aromatic hydrocarbons with UVA light - a pathway leading to the generation of reactive oxygen species, lipid peroxidation, and dna damage. *Int J Environ Res Public Health,* 3**,** 348-54.